



OPEN ACCESS

EDITED BY

Emily G. Mitchell,
University of Cambridge, United Kingdom

REVIEWED BY

Dongjing Fu,
Northwest University, China
Peiyun Cong,
Yunnan University, China
Han Zeng,
Chinese Academy of Sciences (CAS), China

*CORRESPONDENCE

Gaëtan J.-M. Potin
✉ gaetan.jm.potin@outlook.fr

RECEIVED 28 April 2023

ACCEPTED 30 June 2023

PUBLISHED 09 August 2023

CITATION

Potin GJ-M, Gueriau P and Daley AC
(2023) Radiodont frontal appendages from
the Fezouata Biota (Morocco) reveal high
diversity and ecological adaptations
to suspension-feeding during the
Early Ordovician.
Front. Ecol. Evol. 11:1214109.
doi: 10.3389/fevo.2023.1214109

COPYRIGHT

© 2023 Potin, Gueriau and Daley. This is an
open-access article distributed under the
terms of the [Creative Commons Attribution
License \(CC BY\)](#). The use, distribution or
reproduction in other forums is permitted,
provided the original author(s) and the
copyright owner(s) are credited and that
the original publication in this journal is
cited, in accordance with accepted
academic practice. No use, distribution or
reproduction is permitted which does not
comply with these terms.

Radiodont frontal appendages from the Fezouata Biota (Morocco) reveal high diversity and ecological adaptations to suspension-feeding during the Early Ordovician

Gaëtan J.-M. Potin^{1,2*}, Pierre Gueriau¹ and Allison C. Daley¹

¹Institute of Earth Sciences, University of Lausanne, Lausanne, Switzerland, ²Géosciences Rennes, CNRS, UMR 6118, Univ Rennes, Rennes, France

Introduction: The Early Ordovician Fezouata Shale Formation (485–475Ma, Morocco) is a critical source of evidence for the unfolding Great Ordovician Biodiversification Event (GOBE), the largest radiation in animal diversity during the Paleozoic. The Fezouata Shale preserves abundant remains of ancient marine organisms, including hundreds of specimens of radiodonts, a diverse and globally distributed group of stem lineage arthropods that first appeared as raptorial predators during the Cambrian Explosion.

Methods: In this work, we study 121 radiodont frontal appendages from the Fezouata Shale. Frontal appendages are the most commonly preserved body parts of radiodonts, and their well-preserved anatomical characters are crucial for describing taxonomic diversity at the species level, while also providing essential data on mode of life, paleoecology, and feeding behaviour.

Results: Our data allow for a systematic review of suspension-feeding Hurdiidae radiodonts from Fezouata. The genus *Pseudoangustidontus* is recognised as a radiodont and ascribed to Hurdiidae, and a new second species of this genus is identified, *Pseudoangustidontus izdigua* sp. nov. *Aegirocassis benmoulai* is also reviewed and its diagnosis amended with new details of differentiated endites in this appendage. The morphological similarity between both genera allows us to erect *Aegirocassisinae* subfam. nov., which groups together the suspension-feeding hurdiids of the Fezouata Shale.

Discussion: Suspension-feeding radiodont appendages are more abundant than those of sediment sifting or raptorial radiodonts, with the Fezouata Shale showing the highest diversity of suspension-feeding radiodonts in the history of the group. This dominance and diversity of frontal filter-feeding appendages follows the “Ordovician Plankton Revolution”, which started in the upper Cambrian and saw a huge radiation in plankton diversity.

KEYWORDS

Arthropoda, Radiodonta, evolution, frontal appendages, Fezouata Shale Formation, Early Ordovician, GOBE, suspension-feeder

1 Introduction

The Fezouata Shale, located near the city of Zagora, in the central Anti-Atlas in Morocco (figure 1D in Saleh et al., 2018); (Martin et al., 2016a; Saleh et al., 2018; Vannier et al., 2019; Saleh et al., 2021c), is the only Burgess Shale-type *Lagerstätte* known in the Early Ordovician (Tremadocian-Floian) that yields a rich and diverse assemblage of marine organisms (Gutiérrez-Marco et al., 2017; Lefebvre et al., 2018; Saleh et al., 2020a). The Fezouata Shale is a vital data point in understanding the transition between the Cambrian Explosion and Great Ordovician Biodiversification Event (GOBE) (Martin et al., 2016c; Servais et al., 2016; Vaucher et al., 2016; Saleh et al., 2021c; Saleh et al., 2022a). In the Fezouata shale non-mineralized taxa are abundant and preserve soft tissues with microscopic fidelity. The assemblage consists of a mix of the classic Cambrian Explosion fauna, including aglaspids, nektaspids or Radiodonta well known from Cambrian *Lagerstätten* such as the Burgess Shale (Canada), and Paleozoic animals characteristic of the Ordovician and later Paleozoic such as trilobites, orthoceratids, and chelicerates (Van Roy et al., 2015a; Ortega-Hernández et al., 2016; Pérez-Peris et al., 2021a; Pérez-Peris et al., 2021b).

Radiodonta Collins, 1996 is an order of early Paleozoic (Cambrian, Series 2, Stage 3 to Early Ordovician, and possibly to the basal Devonian) marine nektonic stem lineage members of Arthropoda von Siebold, 1848, which were important apex predators in early animal communities (Daley and Budd, 2010; Zeng et al., 2017; Liu et al., 2018; Guo et al., 2019; Pates and Daley, 2019; Potin and Daley, 2023). Subject to many interpretations since their first discovery, they have a particular and disparate morphology (Walcott, 1911; Conway Morris and Whittington, 1979; Collins, 1996). With adults measuring between 10 and 200cm in length (substantially larger than most other nektonic predators at the time) and a host of unique and highly diagnostic morphological characters, for example circular mouthparts and elaborate frontal feeding appendages (Collins, 1996; Van Roy and Briggs, 2011; Daley et al., 2013a; Van Roy et al., 2015a; Cong et al., 2018; Pates et al., 2019; Moysiuk and Caron, 2022; Potin and Daley, 2023), they are distinctive members of early Paleozoic ecosystems. The frontal appendages are the most common body part found in fossil *Lagerstätten*, owing to their high preservation potential, and they provide crucial information about the feeding strategy, which includes raptorial predation, sediment-sifting generalised predation, and suspension feeding (Briggs, 1979; Nedin, 1999; Daley and Budd, 2010; Daley et al., 2013a; Van Roy et al., 2015b; Servais et al., 2016; Pates et al., 2019; Pates et al., 2021a; Potin and Daley, 2023).

Phylogenetic analyses identify four radiodont families globally (Vinther et al., 2014; Lerosey-Aubril and Pates, 2018; Potin and Daley, 2023), only one of which, the Hurdiidae, has so far been identified from the Fezouata Shale (Van Roy and Briggs, 2011; Van Roy et al., 2015b). Hurdiidae are typically characterized by frontal appendages with podomeres that bear long, blade-like spines called endites (Lerosey-Aubril and Pates, 2018; Moysiuk and Caron, 2022; Wu et al., 2022). They first appeared during Cambrian Epoch 2 Age 3, and are abundant, diverse and globally distributed throughout the Cambrian (Zhu et al., 2021). In the Early Ordovician Fezouata

Shale, the two meter long suspension-feeding *Aegirocassis benmoulaï* is the only hurdiid/radiodont taxon formally described from the site (Van Roy et al., 2015b), interpreted as occupying the same ecological niche as some present-day whales or whale sharks (Van Roy et al., 2015b). Other specimens of hurdiids from Fezouata have been identified but no formal taxonomic description provided (Van Roy and Briggs, 2011).

This study focuses on hurdiid frontal appendages from the Fezouata Shale, expanding upon the known diversity and increasing the disparity of known functions at this site. Owing to newly discovered specimens, this paper provides new insight into radiodont evolution, particularly for the family Hurdiidae. The internal taxonomy of the Hurdiidae is re-evaluated with the creation of the suspension-feeding clade Aegirocassisinae, which unites *Aegirocassis benmoulaï* and the genus *Pseudoangustidontus*, here identified as a Hurdiidae. The re-evaluation of *Pseudoangustidontus* results in the separation of *P. duplospineus* and *P. izdigua* sp. nov. The new specimens also provide data on the mineral composition of the frontal appendages fossils, and allows for a new perspective into radiodont ecology and evolution.

2 Geological context

The Fezouata Shale is an Early Ordovician *Konservat-Lagerstätte* of the Anti-Atlas of Morocco (Martin et al., 2016c; Drage et al., 2019; Saleh et al., 2019; Saleh et al., 2020a). This *Lagerstätte* formed on the northern Gondwanan margin at approximately 65° South of latitude, near the Ordovician south polar circle, consequently in a cold-water depositional context (figure 1D in Saleh et al., 2018) (Martin et al., 2016c; Saleh et al., 2018; Drage et al., 2019; Saleh et al., 2019; Saleh et al., 2020a; Saleh et al., 2021c). The sediments were deposited during the tectonic rifting that led to the formation of the Rheic ocean between the Avalonian and Gondwanan paleocontinents (figure 1D in Saleh et al., 2018) (Martin et al., 2016c; Vaucher et al., 2016; Lebrun, 2017; Saleh et al., 2018).

The Fezouata Shale Formation (between 900 and 1000 meters) is mainly composed of argillites and siltstones (Vidal, 1998; Lebrun, 2017; Vaucher et al., 2017). It is a subdivision of “External Feijas Group” which is one of the four big lithostratigraphic units of the Ordovician in modern day Morocco (Martin et al., 2016c). The Fezouata Formation is composed of the lower and upper Fezouata Shale units, which are separated by a surface that corresponds to a glauconitic and ferruginous horizon reflecting a maximum flooding interval (Martin et al., 2016c). Sediments were deposited almost exclusively in environments between the fair-weather wave base and just below the storm weather wave base (Vidal, 1998; Martin et al., 2016c; Vaucher et al., 2016; Saleh et al., 2018; Saleh et al., 2021b).

Several modes of fossilisation have been described for the *Konservat-Lagerstätte* aspects of the Fezouata Shale. Giant radiodont carcasses (e.g. of *Aegirocassis*) are preserved three-dimensionally within large (>1 m) silica-chlorite concretions, resulting from the microbial decomposition of their organic tissues (Gaines et al., 2012; Van Roy et al., 2015b). A similar mechanism led to the preservation of large trilobites from the

temporally and spatially (<50 km) coeval locality of Ouled Slimane (Saleh et al., 2021c). In the second mode, which concerns the great majority of the Fezouata taxa (i.e. smaller mineralised and soft-bodied organisms or tissues, as well as shed exoskeletal remains), fossils are preserved as two-dimensional iron oxide compressions within mudstone (Van Roy et al., 2010; Martin et al., 2016b). These compressed soft-body fossils resulted from burial *in situ* under storm-induced deposits (Vaucher et al., 2016; Lefebvre et al., 2018; Saleh et al., 2018). Pre-burial degradation was slowed by the deposition of a favourable clay mineralogy (Saleh et al., 2019) that allowed for the preservation of decay-prone structures such as internal and cuticularized tissues (Saleh et al., 2020c). It has been shown (Vaucher et al., 2016; Saleh et al., 2020c; Saleh et al., 2021b) that originally these fossils first turned into carbonaceous films and/or were replicated in rapidly forming authigenic minerals particularly pyrite (Saleh et al., 2020c; Saleh et al., 2021b). There are two main intervals of this mode of preservation (figure 1A in Saleh et al., 2018), dated to the Tremadocian and Floian (Vaucher et al., 2016; Lefebvre et al., 2018; Saleh et al., 2018). The lower interval is dated to the terminal Tremadocian based on the graptolite biozone *Sagenograptus murrayi* (previously called *Araneograptus murrayi*) and the beginning of *Hunnegraptus copiosus*, at the top of the lower member of the Fezouata Shale Formation (Martin et al., 2016b; Vaucher et al., 2016; Lefebvre et al., 2018; Saleh et al., 2018; Saleh et al., 2022c). The upper interval dates from the Floian based on the *Baltograptus jacksoni* biozone (figure 1A in Saleh et al., 2018) (Lefebvre et al., 2018; Saleh et al., 2018). The *Konzentrat-Lagerstätte* in the upper member dates to the Middle Floian, probably in the *Azygograptus suecicus* biozone, which formed in a more proximal area of the basin (Martin et al., 2016b; Vaucher et al., 2016). A third mode of preservation yielding non-biom mineralised fossils has also been reported from the upper Floian of the Fezouata Shale, dominated by three-dimensionally preserved sclerotized fragments of large bivalve and/or radiodont arthropods together with brachiopods, echinoderms and graptolites (Saleh et al., 2022c). Fossils in this study derive from the Tremadocian interval of exceptional preservation in the form of two-dimensional iron oxide compressions.

3 Material and methods

3.1 Fossil specimens

This study is based on 112 specimens of frontal appendages belonging to suspension feeding hurdiids found in the Tremadocian (about 478 million years ago), from the exceptionally well-preserved lower member of the Fezouata Shale (Supplementary Table 1) (Martin et al., 2016b; Vaucher et al., 2016). All appendages examined for this study are housed in the collections of the Muséum cantonal des sciences naturelles, département de géologie, Lausanne (MGL), the Peabody Museum of Natural History of the Yale University (YPM), and the Marrakech Collections of the Cadi Ayyad University. The MGL and YPM material has been collected by authorized and academically recognized Moroccan collector Mohamed Ben Moula and his family over the period of 2015 to 2016 (MGL collection), and

between 2009 to 2015 (YPM collection). The MGL fossil collection was purchased with funds from the University of Lausanne and the Swiss National Science Foundation, following all regulations for purchases. The fossil collection was transported to Casablanca and subjected to export approval by the Ministry of Energy, Mines and the Environment of the federal government of the Kingdom of Morocco and approved for shipment to Switzerland on 11.05.2017 (export permits curated with the collection). Fossils were shipped by sea and land to the University of Lausanne, where they are curated as part of the MGL collection. The collections of the Yale Peabody Museum of Natural history were obtained both through collection of specimens by Peter Van Roy during field work, and through purchase using dedicated museum funds for the acquisition of scientific collections. Export permits were obtained through the Moroccan Ministry of Energy, Mines and the Environment, with specimens being transported from Casablanca by sea. In addition, some data come from previous publications and are cited accordingly.

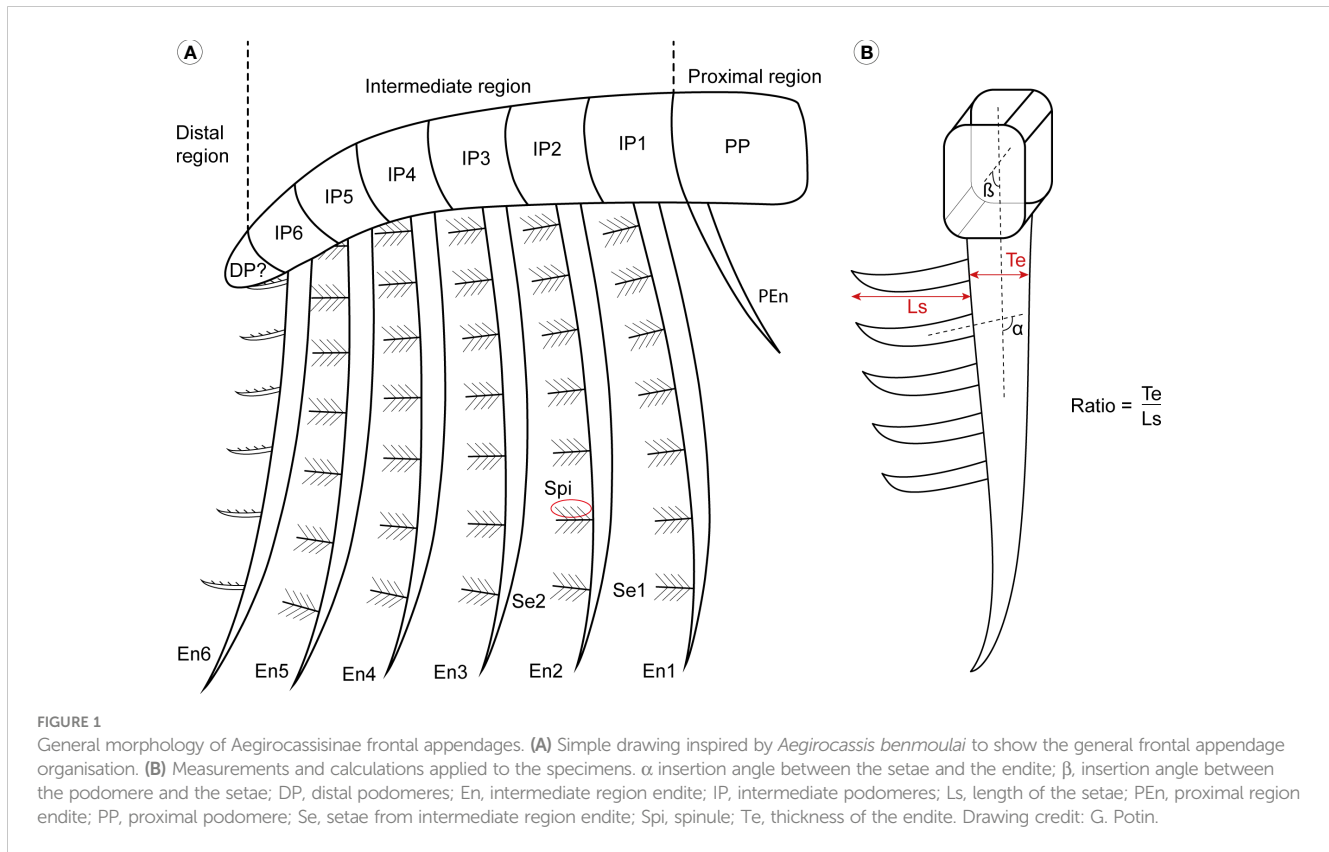
An additional 9 hurdiid radiodont appendages that do not show characteristics of suspension feeding morphology were examined and included in the analyses of proportions of feeding modes found in the Fezouata Shale (see list of specimens in Supplementary Table 1). These taxa, some of which have been previously published with brief descriptions (Van Roy and Briggs, 2011), have morphologies similar to *Hurdia* and *Peytoia*, and their detailed systematics will be the subject of a future study.

3.2 Terminology

In this work we follow the terminology of Potin and Daley (2023) for the anatomical features of the frontal appendages. As exemplified by the nearly complete *Aegirocassis benmoulai* appendages, the overall morphology consist of series of articulated podomeres divided into three regions: the 'proximal region' that usually includes a single podomere with an endite at the distal margin (referred to as the 'base', 'shaft' or 'peduncle' in previous publications, see Supplementary Table S1 in Potin and Daley, 2023); an 'intermediate region' of five or six podomeres that bear elongate blade-like endites; and a 'distal region' of one or several podomeres bearing short endites or no endites at all (Wu et al., 2022; Potin and Daley, 2023) (Figure 1). Endites in all three regions can bear 'auxiliary spines', distributed along the anterior or posterior (or both) margins. In suspension feeding taxa, the thin, densely-packed auxiliary spines of the elongated endites of the intermediate region are called 'setae', to which fine 'spinules' can be attached (Figure 1) (Van Roy et al., 2015b; Lerosey-Aubril and Pates, 2018; Potin and Daley, 2023).

3.3 Specimen examination, Photography, and Illustrations

Specimens were examined with a binocular microscope WILD typ 308700 (X6.4, 16, 40) to identify the microstructures, while camera lucida drawings were made in order to illustrate and record the morphological details. Photos were taken with a Canon 8000D



camera couple with a Canon EFS 60mm 1:2.8, and EOS Utility photo software was used to adjust contrast and sharpness. Fossils were imaged using different lighting conditions, including high and low angle incident and polarised lighting. Drawings and figures were digitised using Wacom Intuos Pro graphic tab, and further prepared with the software Adobe Photoshop and Adobe Illustrator under license to the University of Lausanne. The expression of relief on the drawings corresponds to the method of (Whittington, 1975), with hachures starting on the point of high relief and moving downwards.

3.4 Measurements

Primary measurements (Supplementary Table 2) were made, using digital callipers, of the height, length, and thickness of the major morphological characters (podomeres, endites, setae and spinules), and the angle (α) between a seta and the margin of the endite to which it attaches was also measured. If the angle measure α is more than 90° , the seta is oriented to the ventral margin and, if less than 90° it is oriented to the dorsal margin (Figure 1). A number of morphometric parameters were then calculated using these baseline measurements, for use as quantitative variables that distinguish between genera and species. The first parameter is dimensionless and compares setae length and the thickness of the endite where it is attached, such that the ratio T_e/L_s consist of the endite thickness (T_e) divided by the setae length (L_s) (Figure 1). The ratio is calculated to see if there are differences between the dimensions of endites of the different species, and also if there are some intraspecific differences. To examine the suspension feeding mode of life, primary

measurements was also used to calculate mesh sizes as either the space between the setae, or by the space between the spinules (if they are present), on the elongated endites of the intermediate region. The mesh size measurement allows for an estimate of the size of the plankton that can be captured during suspension feeding (Robison and Richards, 1981; Vinther et al., 2014).

3.5 Analyses

A study of the mode of insertion of the setae on the 6th endite of *Aegirocassis benmoulai* and *Pseudoangustidontus izdigua* sp. nov. was used to test for a significant difference of insertion angle between these taxa. The 6th endite was chosen because is the endite that clearly showed the insertion angle in the highest number of specimens, giving a total sample size of 29 appendages (Supplementary Table 3). Using PAST version 4 (Hammer et al., 2001), a Shapiro-Wilk test for normality was conducted, followed by a two-sample Kolmogorov-Smirnov test with Monte Carlo permutation to compare the overall two-sample distribution with their cumulative probability distribution (Hammer and Harper, 2008; Antcliffe et al., 2019). Violin and box plot were made to compare the results of the two insertion modes, which were then modified for the figures using Adobe Illustrator.

RStudio was used to generate a pie chart by using the function pie in order to visualize the proportion of the different radiodont taxa found in the Fezouata Shale.

The graph showing the size of particles captured by suspension-feeding radiodonts has been modified from (Vinther et al., 2014).

Data concerning *Pahvantia* mesh size were exported from (Lerosey-Aubril and Pates, 2018), and the data for *Tamisiocaris* derive from (Van Roy et al., 2015b). Our data come from a selection of well-preserved specimens, showing multiple well-preserved setae and/or spinules associated with the five first endites of the intermediate region (see Supplementary Table 2).

3.6 X-ray microtomography

X-ray computed microtomography (μ CT) was conducted on the *Pseudoangustidontus izdigua* sp. nov. paratype MGL 103606 at the Institute of Earth Sciences, University of Lausanne, using a Skyscan 1273 CT scanner (Bruker-microCT, Kontich, Belgium) operating under a voltage of 130 kV and a current of 115 μ A. Projections were collected with a pixel size of 40 μ m using a rotation step of 0.15° over 360° (around the vertical axis), a 1005 ms exposure time with 3 averaged images per projection, and a 2.0 mm thick copper filter. Tomographic slices were reconstructed using NRecon v. 1.7.1.0 software (SkyScan 1273; Bruker-microCT, Kontich, Belgium), using a beam hardening correction of 20%, a ring artifact correction of 10, and a smoothing of 1. Segmentation and 3D rendering were performed using 3D Slicer (<https://www.slicer.org/>) on a slightly reduced version of the dataset (2×2×2 binning, resulting in a voxel size of 80 μ m) to facilitate 3D data processing.

3.7 Raman microspectroscopy

Raman microspectroscopy was performed on MGL 103593b, 103606b, 103613a and 103596a at the Institute of Earth Sciences, University of Lausanne, using a Horiba Jobin Yvon LabRAM 800 HR spectrometer in a confocal configuration, equipped with an Ar+ laser (532 nm) excitation source and an electron multiplying charge-coupled device (EMCCD). Spectra were collected at constant room temperature, directly on the sample surface, by focusing the laser beam with a 400 μ m confocal hole using a long working distance ×50 objective (NA = 0.70). This configuration provided a \approx 4 μ m spot size for a laser power delivered at the sample surface below 1 mW. Light was dispersed using a 1800 gr/mm diffraction grating. Mineral identification was carried out using references from the RRUFF database (<https://rruff.info/>).

3.8 Elemental mapping

Synchrotron micro X-ray fluorescence (μ XRF) major-to-trace elemental mapping of MGL 103593b was performed at the DiffAbs beamline of the SOLEIL synchrotron source (France), using a monochromatic beam of 18 keV, selected for excitation of all chemical elements of the periodic table commonly present in geological materials, i.e. up to uranium (physically speaking, 18 keV X rays lead to the excitation of K-lines up to yttrium and L-lines from cadmium to uranium). In practice, however, the experiment is performed in air and as such detection of light

elements up to phosphorous is not possible or very limited. In order to map the specimen with a high resolution, the beam was reduced down to a diameter of 50 μ m using a molybdenum pinhole. The sample was mounted on a scanner stage allowing 90 mm movements (in both horizontal and vertical directions) with micrometre accuracy, and orientated at 45° to the incident beam. XRF was collected using a 4-element silicon drift detector (SDD, Vortex ME4, Hitachi High-Technologies Science America, Inc., total active area: 170 mm²) oriented at 90° to the incident beam, in the horizontal plane. A two-dimensional spectral image, i.e. an image for which each pixel is characterized by a full XRF spectrum, was collected on the fly (Leclercq et al., 2015) over most the specimen at a 70 μ m lateral resolution with a 25 ms dwell time (effective counting time 23 ms). The obtained dataset comprises 1'267'716 spectra (1068×1187 pixels; covering an area of 75×83 mm²). μ XRF elemental distributions presented in Figure 2C were produced through the collection of integrated intensities (sum of the four-elements XRF detector) within 100-eV-wide regions of the spectra corresponding to emission from elements of interest. Average μ XRF spectra and main elemental contributions shown in Figure 2D were extracted and obtained using the PyMCA data-analysis freeware (Solé et al., 2007).

3.9 Abbreviations

Systematic abbreviations. a/b, indicates that there are part and counter-part; NC, indicates there is only one side.

Anatomical abbreviations. See Figure 1.

Institutional abbreviations. MGL, Musée Cantonal de Géologie Lausanne, Lausanne, Suisse; NMS, The National Museums of Scotland, Edinburgh, Scotland; NMW, National Museum Wales, Cardiff, Wales; YPM, Yale Peabody Museum of Natural History, Yale, USA.

4 Results

This report provides new anatomical data for two previously published taxa, *Aegirocassis benmoulai* and *Pseudoangustidontus duplospineus*, and describes one new species *Pseudoangustidontus izdigua*. Moreover, we erect the new subfamily Aegirocassisinae to include these two genera, uniting the suspension-feeding radiodonts from the Fezouata Shale by their shared morphological adaptations for that mode of life.

4.1 Preservation

Mineral characterization using Raman microspectroscopy of four of the specimens investigated herein confirm an iron oxide composition for these fossils, in line with previously published reports on the mode of preservation of these compressed non-mineralised fossils (Vaucher et al., 2016; Lefebvre et al., 2018; Saleh et al., 2018; Saleh et al., 2019; Saleh et al., 2020a; Saleh et al., 2020b; Saleh et al., 2020c; Saleh et al., 2021b). Quartz and clay minerals are the

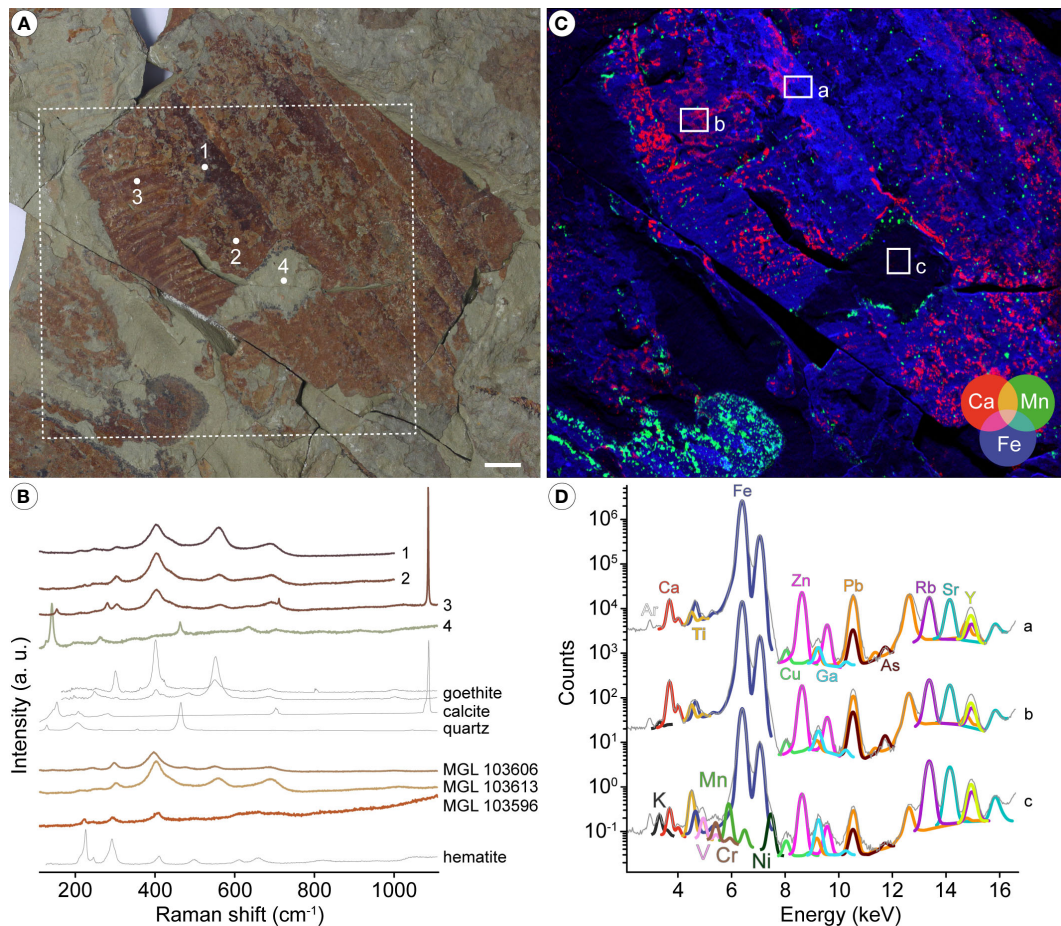


FIGURE 2

Mineralogical and elemental composition of radiodont frontal appendages from the Fezouata Shale. (A) Optical photograph of *Aegirocassis benmoulai* (Van Roy et al., 2015b) specimen MGL 103593b. (B) Raman microspectroscopy of MGL 103593b (spectra 1 to 4 from the corresponding points in A), as well as of *Pseudoangustidontus izdigua* sp. nov. paratype MGL 103606b, and of *Pseudoangustidontus duplospineus* (Van Roy and Tettie, 2006) specimens MGL103613a and 103596a. Mineral reference spectra are taken from the RRUFF database; goethite is represented by two spectra collected using directions of polarization of the laser of 90° (top) and 0° (bottom). (C) False-color overlay of calcium (red), manganese (green), and iron (blue) distributions from the dotted white box in A. (D) Average μ XRF spectra and main elemental contributions from the corresponding white boxes in C. Scale bars: 1cm. Image credit: P. Gueriau.

main constituents of the surrounding sedimentary mudstone matrix (Figures 2A, B). Characteristic spectral features identify the oxides as goethite (α -FeO(OH)) in MGL 103593 (*A. benmoulai*), MGL 103606 (*P. izdigua* sp. nov.) and MGL 103613 (*P. duplospineus*), and as hematite (α -Fe₂O₃) in MGL 103596 (*P. duplospineus*) (Figure 2B), highlighting variability in the formation and/or deposition of the iron oxides. The composition of MGL 103593 also locally includes calcite (Figures 2A, B), which is present over many regions of the specimen as evidenced by the distribution of Ca obtained using μ XRF major-to-trace elemental mapping (Figure 2C). The random distribution pattern of calcite and the fact that carbonates from the matrix and from the skeletal elements of animals such as echinoderms are known to have dissolved under the action of modern water circulations (Saleh et al., 2020b; Saleh et al., 2021b) suggest that these phases deposited recently and therefore do not represent any biomineralization of the cuticularized tissue. μ XRF spectra further indicate that the iron oxides have incorporated trace metals, particularly Zn, As and Pb (Figure 2D). Altogether, the geochemical data indicate that preservation of the material studied herein follows the taphonomic

model proposed for other organisms preserved as two-dimensional iron oxide compressions within mudstone (Saleh et al., 2021b). Consequently, the lack of biomineralized structures within the studied appendages should be treated as a real absence, whereas the lack of soft cellular structures in direct contact with seawater is most likely taphonomic (Saleh et al., 2020a; Saleh et al., 2021a; Saleh et al., 2021b). By distinguishing between real biological and taphonomic absences, it becomes possible to identify and account for the biases that may have influenced the recorded faunal composition. In the context of the current study, this distinction provides a more reliable and comprehensive understanding of the original composition of the radiodont appendage (for similar consideration in the Chengjiang Biota, see Saleh et al., 2022b).

4.2 Dimorphism analysis

A new morphology of Hurdiidae endite is identified and well preserved on 29 specimens, some of which represent isolated

specimens of a single endite and some of which are associated with more endites and podomeres of the rest of the appendage. Consequently this either represents a new species of Hurdiidae or it represents a dimorphic endite from a known taxon. Detailed study of the most complete specimens of (MGL 103599, MGL 103604, MGL 103614, YPM IP 523428) allows us to confirm that dimorphism of endites is the most likely solution to this errant morphology. The dimorphic endite corresponds of the 6th endite of the intermediate region of *Pseudoangustidontus izdigua* sp. nov. and *Aegirocassis benmoulai*.

The dimorphic endites from *Aegirocassis* and *Pseudoangustidontus* are similar, however the insertion of the setae on the endite and the presence or absence of spinules allow for distinction of the dimorphic endites between the taxa. Three variables were revealed as crucial for this distinction: the insertion mode (simple or triangle) and the angle of insertion (between 75° and 135°) of setae on the endites, and the spinules (present or absent). Given that the distribution of measurements of the angle of insertion for both simple (Shapiro-Wilks test, $n=20$, $W=0.8184$, $p=0.001649$) and triangular (Shapiro-Wilks test, $n=9$, $W=0.773$, $p=0.01001$) insertions were significantly different from normal, a two-sample Kolmogorov Smirnov test with a Monte Carlo permutation was used to determine if there was a significantly different angle of insertion associated with the two insertion modes (Figure 3). It was found that there is a significantly higher insertion angle observed for setae with a simple insertion on the endite (between 100° and 135°) as compared to those with a triangular insertion (75° and 92°) (two sample Kolmogorov-Smirnov test, $n=35$, $p=0.001$). Moreover, all the specimens showing spinules attached to the setae correspond to those that have a simple insertion of 100° and 135° (Supplementary Table 3). These results allow us to say that there are

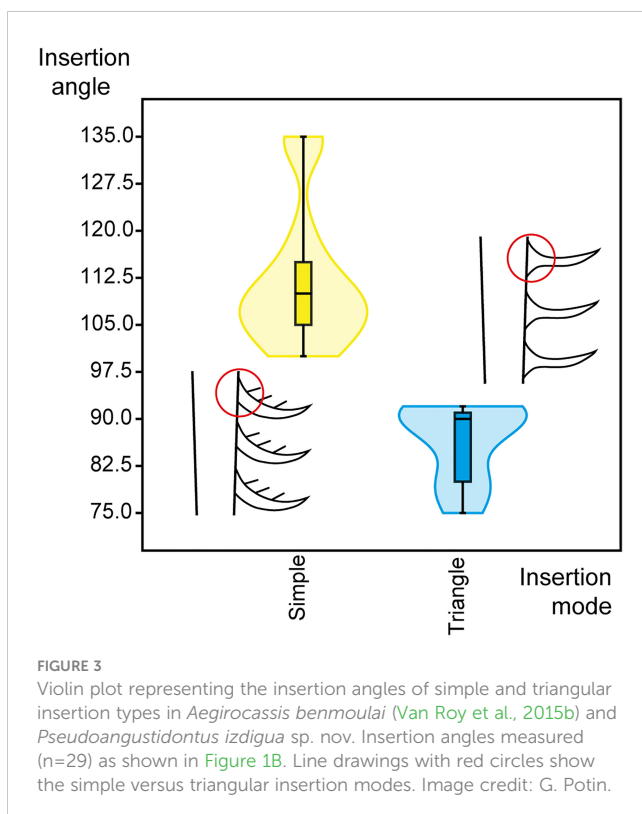
two morphotypes of the dimorphic endites. Owing to the most complete specimens YPM IP 523428, MGL 103599 and MGL 103614 for *Aegirocassis benmoulai* and MGL 103604 for *Pseudoangustidontus izdigua* sp. nov., we are able to associate the two morphotypes to these two taxa. The setae of the 6th endite of *Aegirocassis benmoulai* bear spinules and have simple insertions with angles ranging between 100° and 135°, except in specimens such as MGL 103593 that likely lost them taphonomically. The second morphotype is associated with *Pseudoangustidontus izdigua* sp. nov., where the 6th endite has setae attached with a triangle insertion of between 75° and 92°, none of which shows spinules. There is no specimen complete enough to show the dimorphic endite morphotype in *Pseudoangustidontus duplospineus*.

4.3 Mesh size

The mesh size calculation was made using measurements from the five first endites of the intermediate region of the frontal appendages. The mesh size of *Aegirocassis benmoulai* was measured for eleven specimens (MGL 103594, MGL 103600, MGL 103601, MGL 103627, MGL 103634, MGL 103665, MGL 104310, YPM IP 523428, YPM IP 525217, YPM IP 527123, YPM IP 527125) as these specimens show sufficient spinules preservation to allow measurements and calculation of mesh size, giving a mean of 0.56mm. For the species *Pseudoangustidontus duplospineus* measurements were possible on all specimens ($n=7$) (MGL 102360, MGL 103596, MGL 103609, MGL 103612, MGL 103613, MGL 104332, NMS G.2005.119.1) giving a mean of 0.49mm. Finally, *Pseudoangustidontus izdigua* sp. nov. has a mean of 0.51mm based on eighteen specimens (MGL 103027, MGL 103603, MGL 103604, MGL 103606, MGL 103607, MGL 103611, MGL 103616, MGL 103621, MGL 103622, MGL 104052_1, MGL 104101, MGL 107733, YPM IP 226560, YPM IP 226561, YPM IP 517614, YPM IP 517616, YPM IP 524840, YPM IP 525219). These data were plotted on the graph showing the size of particles captured by suspension-feeding radiodonts (Supplementary Table 2), modified from Vinther et al. (2014), giving a mesoplankton (0.2-20mm) size range of prey for both *Pseudoangustidontus* species and *Aegirocassis*.

4.4 Feeding strategy proportions

A total of hundred and twenty-one frontal appendages specimens were studied of which seventy-eight were possible to identify to species level, yielding forty three *Aegirocassis benmoulai*, seven *Pseudoangustidontus duplospineus* and twenty-eight *Pseudoangustidontus izdigua* sp. nov. A further nine specimens could be confidently assigned to the genus *Pseudoangustidontus* but not allocated to a species. There are a further eight specimens that can be allocated to the broader Aegirocassisinae subfam. nov. that are suspension-feeding radiodonts from Fezouata but without allocation to a genus. Finally, there are nine sediment-sifter radiodont appendages from the Hurdiidae family. The total number of suspension-feeding specimens is therefore 112 out of



121 specimens ($\approx 92.6\%$), whereas only $\approx 7.4\%$ of the radiodont appendage specimens are non-suspension-feeding appendages (Supplementary Table 1).

5 Systematic paleontology

Super-phylum Panarthropoda Nielsen, 1995

Phylum (stem-group) Arthropoda von Siebold, 1848

Order Radiodonta Collins, 1996

Family Hurdiidae Lerosey-Aubril and Pates, 2018

Type genus: *Hurdia* Walcott, 1912

Other genera included: *Aegirocassis* Van Roy et al., 2015b, *Buccaspinea* Pates et al., 2021b, *Cambroraster* Moysiuk and Caron, 2019, *Cordaticaris* Sun et al., 2020a, *Pahvantia* Robison and Richards, 1981, *Peytoia* Walcott, 1911, *Pseudoangustidontus* Van Roy and Tetlie, 2006, *Stanleycaris* Caron et al., 2010, *Titanokorys* Moysiuk and Caron, 2021, *Ursulinacaris* Pates et al., 2019.

Questionably: *Schinderhannes* Kühl et al., 2009

Emended diagnosis: Radiodonts with frontal appendages composed of proximal, intermediate, and distal regions: proximal region comprising one or more podomeres a single or no endites; intermediate region composed of at least five podomeres that are usually twice as high as they are long, and bearing paired or unpaired endites longer than podomere heights; distal region characterized by podomeres reduced in height, length, or both, bearing short or no endites. Endites in the form of thin or thick blades, not alternating in size between odd and even podomeres, typically curved towards the appendage distal tip, and bearing auxiliary structures (spines or setae) projecting from their anterior margins only. Oral cone comprises four large plates at right angles to each other. Large tripartite cephalic carapace extending about as long as half the length of the rest of the body, consisting of a large central element with tapering anterior and notched or flanged postero-lateral margins, flanked by a pair of slightly smaller ovoid or lenticular lateral elements with or without posterior notches. Body bearing two sets of flaps, dorsally and ventrally located, on each main body segment (Emended from Moysiuk and Caron, 2022).

Subfamily Aegirocassisinae subfam. nov.

Figures 4–9.

Etymology: In recognition of *Aegirocassis benmoulai* species, the first recognised member of this group.

Included taxa: *Aegirocassis* Van Roy et al., 2015b, *Pseudoangustidontus* Van Roy and Tetlie, 2006.

Diagnosis: Hurdiids with multisegmented anterior frontal appendages comprising at least 6 podomeres in the intermediate region. The 6 podomeres of the intermediate region bear one endite each, 6 to 10 times longer than the podomere height. The first 5 most proximal endites bear thin setae (less than 1 mm in width, but at least as long as the endite thickness), either single or in pairs, with a triangle insertion to the endite. The 6th most distal endite is dimorphic in bearing curved setae thicker (more than 1 mm wide) but shorter as compared to the setae of the 5 first endites. The tip of all endites is curved toward the inner margin. The distal region of

the appendage is short, consisting of only a few podomeres, possibly bearing a terminal spine.

Remark: All members of Aegirocassisinae had a suspension-feeding ecology, but it does not include all radiodonts interpreted as having a suspension-feeding paleoecology (i.e. *Tamisiocaris* and the possible *Pahvantia*, *Cambroraster*, *Echidnacaris briggsi*). So far, it only includes suspension-feeding radiodonts from the Fezouata Shale. It is named in recognition of *Aegirocassis benmoulai* and not *Pseudoangustidontus* because the latter was not definitively considered to be a radiodont before this study. So far, no proximal podomere has been observed in *Pseudoangustidontus*, and the distal appendage region in *Aegirocassis* and *Pseudoangustidontus* remain poorly known.

Genus *Aegirocassis* Van Roy et al., 2015b

Emended diagnosis for genus and species: Aegirocassisinae with tripartite frontal carapace having a central element at least as long as trunk, with an axial carina, pointed tip, rounded posterior margin and narrow down turned postero-ventral triangular extensions tapering towards rear and overlapping the lateral carapace elements dorsally. Lateral carapace elements oval, with rounded antero-dorsal expansion and longitudinal carina just below midline. Multisegmented anterior appendages consisting of seven podomeres. Proximal podomere longest, with one shorter, comb-like endite proximally. Succeeding six intermediate region podomeres bearing a single elongate, inward-angled endite that is 7 to 10 times longer than the podomere height. First five endites of the intermediate region bearing a single row of setae that are at least twice the length of the endite thickness (ratio $T_e/L_e > 0.5$), each adorned with spinules in a 'V' orientation. The sixth intermediate endite dimorphic and bearing a single row of setae with a simple insertions oriented ventrally with an angle of 100° to 135° from the endite axis. Setae bearing single spinules. Terminal podomere stout, with pointed tip. Flat, broad trunk of 11 segments attaining maximum width at third segment and tapering to a blunt tip. Two pairs of non-overlapping flaps per segment: dorsal flaps pointed with recurving anterior and posterior margins, width about 13 the length of their attachment; ventral flaps narrow, triangular, width about 1.53 the length of their attachment. Continuous band of dorsal setal blades attached to base of each pair of dorsal flaps, traversing the trunk (Emended from Van Roy et al., 2015b).

Type species: *Aegirocassis benmoulai* Van Roy et al., 2015b.

Remark: The orientation of the setae in the first 5 endites from the intermediate region are not relevant because they are flexible.

Aegirocassis benmoulai Van Roy et al., 2015b

v. 2015b *Aegirocassis benmoulai* sp. nov. Van Roy et al.: figures 1–3; Extended data figures 1–7.

2015a *Aegirocassis benmoulai* Van Roy et al.; figure 3.

Figures 2A, C, 4, 9A; Supplementary Figures 1, 2A, B.

Holotype (published): YPM IP 237172,

Paratypes (published): YPM IP 522227, YPM IP 527123, YPM IP 527125,

Plesiotypes: MGL 103593, MGL 108059, YPM IP 523428 (was published as additional material),

Published additional materials: YPM IP 523423, YPM IP 523425, YPM IP 523810, YPM IP 525217, YPM IP 527124, YPM IP 531183,

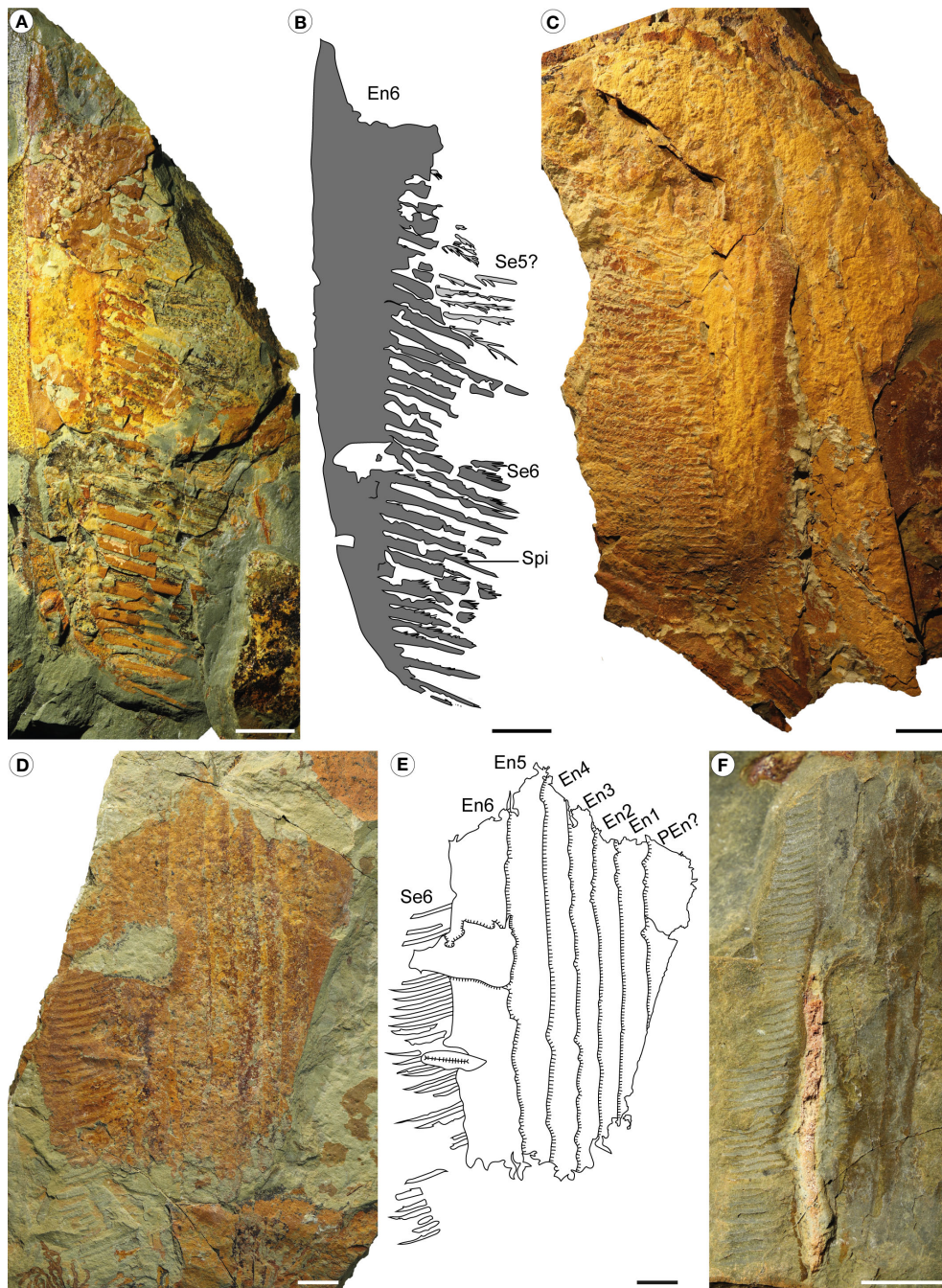


FIGURE 4

Aegirocassis benmoulai from the Fezouata Shale Formation, *Sagenograptus murrayi* biozone, Morocco. (A, B) YPM IP 523428 (plesiotype), showing the 6th endite showing setae and spinules, with the setae of one the 5 other intermediate region endites. (A) Picture under polarized filter. (B) Camera lucida drawing. (C) MGL 103594, picture under polarized filter of intermediate region podomeres and two of the 5 first intermediate region endite, with setae and pair of spinules. (D, E) MGL 103593 (plesiotype), showing the 6 intermediate region endites, the 6th one showing the setae. (D) Picture under polarized filter. (E) Camera lucida drawing. (F) MGL 103614, picture under polarized filter of the endites 4, 5 and 6 from the intermediate regions showing setae and spinules. Abbreviations: same as Figure 1. Scale bars: 1cm. Images and drawings credit: G. Potin

Additional material: MGL 103017, MGL 103594, MGL 103595, MGL 103598, MGL 103599, MGL 103600, MGL 103601, MGL103602, MGL 103608_1, MGL 103614, MGL 103615, MGL 103618, MGL 103620, MGL 103627, MGL 103628, MGL 103629, MGL 103630, MGL 103631, MGL 103633, MGL 103634, MGL 103635, MGL 103636, MGL 103665, MGL 104052_2, MGL 104310, MGL 104322, MGL 107387, MGL 107718, MGL 107912, MGL

107914, MGL 107915, MGL 108047_2, MGL 108053, MGL 108054, MGL 108056, MGL 108058, MGL 108061, MGL 108062, YPM IP 521575, AA.BIZ22.OI.4.

Locality: Specimens collected from outcrops in the Ternata plain, c. 18 km NW of the city of Zagora (Morocco) and c. 6 km NNE of the village of Beni Zouli. GPS coordinates are curated with specimens.

Horizon and age: Lower Fezouata Shale, Late Tremadocian, *Sagenograptus murrayi* biozone.

Diagnosis: As for the genus.

Description: Most of the specimens are incomplete, but together contribute to the overall description. Measurements and quantitative data can be seen in [Supplementary Table 2](#).

MGL 103594 a/b ([Figure 4C](#); [Supplementary Figures 1A, B](#)) shows many of the typical features of the appendages of this taxon as previously described by [Van Roy et al. \(2015b\)](#). It consists in one proximal podomere bearing a short endite and five intermediate podomeres, with the last one being fragmented. The podomeres are curved along the dorsal margin. Endites, setae and spinules are most complete on the first two podomeres (IP1 & IP2) in the intermediate region, which shows the typical anatomy of a single row of long setae on the anterior margin with spinules oriented towards the inner margin. Endites and setae are not completely preserved, but there are at least thirty-two setae and they are >2cm in length ([Figure 4](#)).

YPM IP 523428NC, (already mentioned in [Van Roy et al., 2015b](#)) is here reinterpreted as showing the dimorphic endite on the 6th podomere of the intermediate region endite, only the most distal part, bearing thick, short and curved setae ([Figures 4A, B](#)), some of which show multiple single spinules on their dorsal margin. Setae of another endite (that we cannot see because the more distal endites is overlapping it) are also visible, showing setae that bear rare spinules in the “V” orientation, thus confirming that the dimorphic endite is found in the same appendage as other endites with the previously described morphology. Other specimens also show the newly identified dimorphic endite.

MGL 103593a/b exhibits the 6 endites of the intermediate region, overlapping each other, and possible a short endite of the proximal region ([Figures 4D, E](#)). The 6th endite is the only one showing setae, which are reduced and measure less than 20mm in length, but which are relatively thick (more than 1mm).

MGL 108059NC ([Supplementary Figure 1D](#)) is also one of the rare specimen showing the two morphologies of the setae. It consist of three long (146.7 mm) fragmented intermediate region endites (the 4th, 5th and 6th). Endite 4 exhibits rare thin setae (length not complete), with a few spinules visible that are arranged in a “V”. Endite 6 has several thick setae attached, with only a few spinules preserved.

MLG 103614a/b ([Figure 4F](#); [Supplementary Figures 1E, F](#)) is a small specimen consisting of endites 4 to 6 of the intermediate region. The dimorphic 6th endite bears curved and thick setae that have single spinules on the dorsal margin. Endites 3, 4 and 5 show the triangular insertion points of the thin setae, but the setae are mostly covered by endite 6.

MGL 103599a/b ([Supplementary Figure 1G](#)) consists of endites 3 to 6 of the intermediate region, with visible long and thin setae bearing rare spinules on endites 4 and 5, and thicker setae on the 6th endite, with a simple insertion of 110°.

The largest specimen, MGL 103620NC, consists in endites 4 to 6, with endite 6 exhibiting fragmented setae. Despite the fact that it is fragmented, this endite measures 250mm in length.

Comments: First named *Aegirocassis benmoulae* in [Van Roy et al. \(2015b\)](#), a nomenclature correction in [Van Roy et al. \(2015a\)](#)

renamed the species *Aegirocassis benmoulae*. The new material matches the previous published description, except for the new features described for the dimorphic endite. The holotype YPM 237172 is the only non-frontal appendage specimen listed above, so it is not used in the statistics. YPM IP 523428 was considered as [Supplementary Materials](#) in [Van Roy et al. \(2015b\)](#) (Extended Data figure 6) but in this paper, it is considered as a plesiotype owing to the new morphological characters ([Supplementary Table 1](#)). The isolated setae from YPM IP 523428 have been identified as belonging to the same specimen because they are oriented in the exact same direction, and covered by the visible endite.

Genus *Pseudoangustidontus* [Van Roy and Tetlie, 2006](#)

Diagnosis (emended): Aegirocassisinae with appendages characterised by the first 5 intermediate region endites bearing paired setae that are thin, at least as long as the endite thickness, and not bearing any spinules. Endites have a carina on the outer margin. The 6th intermediate, dimorphic, endite bearing single curved setae, shorter (around twice the endite thickness length) with a triangle insertion and oriented ventrally with an angle of 75° to 90° from the endite axis (Modified from [Van Roy and Tetlie, 2006](#)).

Type species: *Pseudoangustidontus duplospineus* [Van Roy and Tetlie, 2006](#)

Pseudoangustidontus duplospineus [Van Roy and Tetlie, 2006](#)

2006 *Pseudoangustidontus duplospineus* [Van Roy and Tetlie](#): figures 3, 4.

[Figure 5](#).

Holotype: NMS G.2005.119.1

Additional material: MGL 102360, MGL 103596, MGL 103609, MGL 103612, MGL 103613, MGL 104332.

Locality: Specimens collected from outcrops in the Ternata plain, c. 18 km NW of the city of Zagora (Morocco) and c. 6 km NNE of the village of Beni Zouli. GPS coordinates are curated with specimens.

Horizon: Lower Fezouata Shale, end of the Tremadocian, *Sagenograptus murrayi* biozone. According to [Van Roy and Tetlie \(2006\)](#), Upper Fezouata Shale, from Middle Arenig to end of the Floian.

Diagnosis (emended): *Pseudoangustidontus* with paired setae alternating in length short/long. Shorter setae around the same length as endite thickness/height and long ones at least twice the length of endite thickness/height (Modified from [Van Roy and Tetlie, 2006](#)).

Description: MGL 103596 a/b ([Figures 5A, B](#)) consists of a fragmented endite of a frontal appendage. The endite has a carina on the outer margin with a thickness of 0.5 mm. The setae are organized in pairs but is only visible on some setae owing to the incomplete preservation. Longest setae are almost 3 times longer than the small ones. MGL 103613 a/b ([Figure 5C](#)) is a long endite. The endite extremity is curved inwards. Paired setae are badly preserved, but are in pairs, with alternation in length visible for 3 of them.

Pseudoangustidontus izdigua sp. nov.

Life Science Identifier (LSID): urn:lsid:zoobank.org:act:53D86B6F-65DF-490C-B8EB-BEC30A2C49D1

v. 2010 spinose arthropod appendage [Van Roy et al.](#): figure 11. [Figures 6–8, 5B](#); [Supplementary Figure 2A](#).

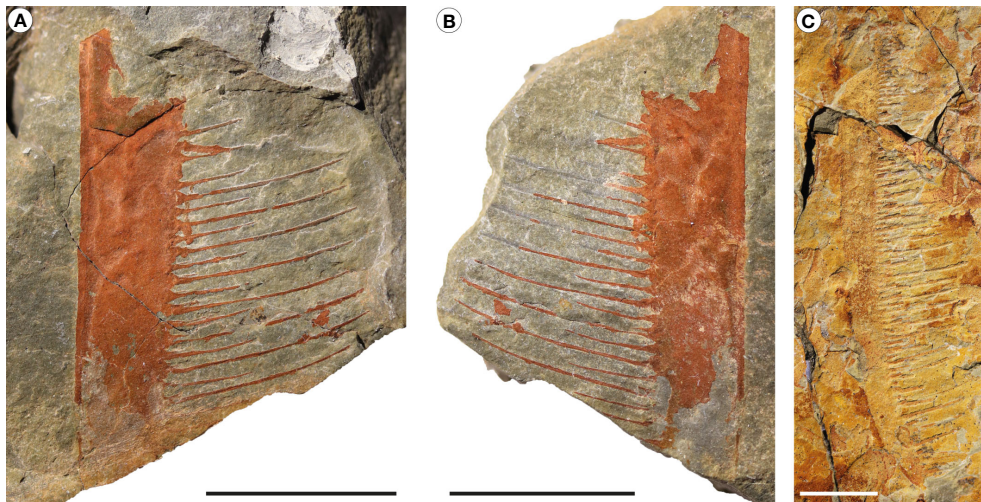


FIGURE 5

Pseudoangustidontus duplospineus from the Fezouata Shale Formation, *Sagenograptus murrayi* biozone, Morocco. (A, B) MGL 103596, picture under polarized filter of a single endite showing the alternative sizes of the paired setae. (A) Part. (B) Counterpart. (C) MGL 103613, picture under polarized filter of a single endite showing the alternative sizes of the paired setae. Scale bars: 1cm. Images credit: G. Potin.

Etymology: The species *izdigua* refers to the Tamazight language translation for filter, *izdigue*, as this species is considered to be a suspension-feeding radiodont.

Holotype: MGL 108047_1

Paratypes: MGL 103606, MGL 104052_1, YPM IP 226559,

Additional material: MGL 102153_2, MGL 102181_2, MGL 102237_2, MGL 103027, MGL 103597, MGL 103603, MGL 103604, MGL 103607, MGL 103608_2, MGL 103611, MGL 103616, MGL 103621, MGL 103622, MGL 104101, MGL 104227, MGL 104414, MGL 107733, YPM IP 226560, YPM IP 226561, YPM IP 517614, YPM IP 517616, YPM IP 518318, YPM IP 524840, YPM IP 525219, YPM IP 532033.

Locality: Specimens collected from outcrops in the Ternata plain, c. 18 km NW of the city of Zagora (Morocco) and c. 6 km NNE of the village of Beni Zouli. GPS coordinates are curated with specimens.

Horizon: Lower Fezouata Shale, Late Tremadocian, *Sagenograptus murrayi* biozone.

Diagnosis: *Pseudoangustidontus* with frontal appendage bearing endites with setae that are all the same length (no long/short alternation). The length of the setae is at least twice as long as the endite thickness.

Description: MGL 108047_1 NC (Figure 6; Supplementary Figure 2A) is divided in two parts, a lower (Figure 6C) and an upper part (Figures 6D, E), separated by the overlapping specimen MGL 108047_3. This specimen consists of four podomeres (visible in the upper part), probably from the intermediate region. It exhibits at least 5 intermediate region endites (the 2nd to the 6th) visible in the lower part. Those endites all have attachment sockets, in which setae would have attached. No setae are present in the lower part of endites 2 to 6. Endite 6 has several thick, short and curved setae attached (19.8mm in length and 2.7mm width). Their

insertion mode is obscured by the visible sockets and the patchy preservation. In the upper part, there are three visible endites in the intermediate region, but the overlying setae make it impossible to determine which of the five non-dimorphic endites they are and to which podomeres they are associated. These endites in the upper part bear long and thin setae (29.9mm long and 0.2mm in width), and in several places the paired attachment of setae is clearly visible. The insertion mode of these setae is triangular, and insertion sockets are visible for some setae (Figures 6D, E).

Specimen MGL 103606a/b/c/d consists of 6 intermediate region endites (Figure 7). MGL 103606a/b/c shows that endites 1 to 5 have setae in pairs, which are long and thin with equal length and 103606c/d shows that the 6th endite bears single curved setae that are shorter and thicker, with a triangle insertion of 90°. On MGL 103606a/b the carina on the outer margin can be distinguished. There is an unidentified carapace fragment of 3mm diameter preserved amongst the setae of the endites 1 and 2 of this specimen.

Specimen MGL 104052_1 a/b (Figures 8A–E) consist of 6 podomeres, at least 4 of which are from the intermediate region because they are associated with long endites bearing long and thin setae in pairs that have a regular non-alternating length. The other endites cannot be identified because incompleteness of the appendage prevents determining an orientation. The podomeres are preserved oblique to the sediment surface and in section, showing a U-shaped outline that is 12 mm in width.

YPM IP 226559 (Figure 8F) consist of 6 endites from the intermediate region, on which the 6th endite clearly possesses thick and short setae that have the triangle insertion of 90°. Some of the other endites show the triangle base of the paired setae, which are occasionally fragmented.

MGL 103611NC (Figure 8G), the smallest specimen, consists of a fragmented curved endite bearing setae in pairs. The tip is curved.

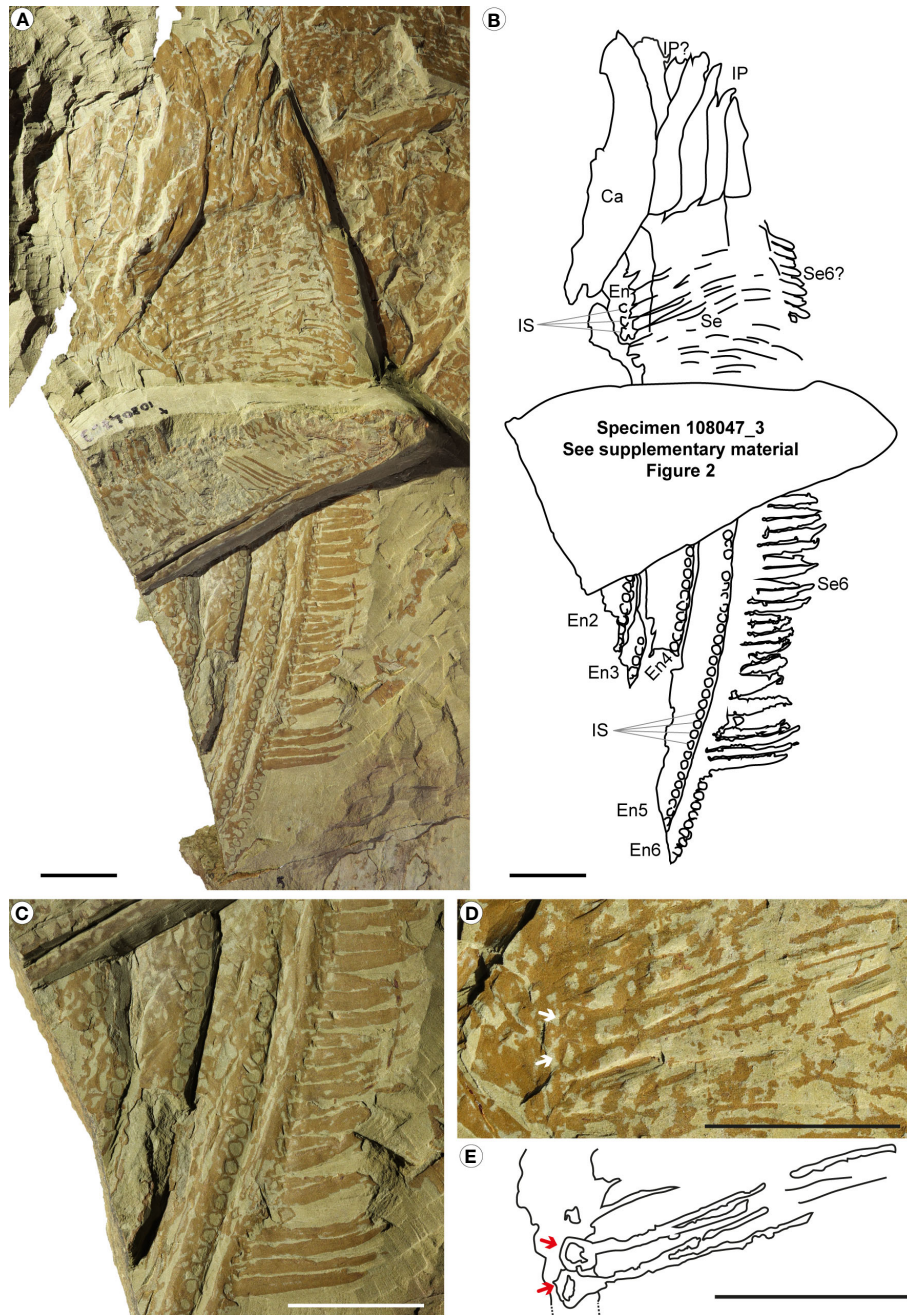


FIGURE 6
Pseudoangustidontus izdigua, MGL 108047_1 (holotype) from the Fezouata Shale Formation, *Sagenograptus murrayi* biozone, Morocco. **(A, B)** Entire specimen showing 4 intermediate region podomeres, with, at least 5 intermediate region endites (the 2nd to the 6th) with the two morphologies of setae and the insertion sockets. **(A)** Picture under polarized filter. **(B)** Camera lucida drawing. **(C)** Picture under polarized filter of the lower part of the specimen with endites 2 to 6 of the intermediate region, all showing the insertion sockets and the 6th endite showing the setae. **(D)** Picture under polarized filter of the upper part of the specimen with 4 (maybe 5) podomeres, with the 6th endite of the intermediate region with setae, and non-recognizable intermediate region endites, some showing the pairs of setae and some insertions sockets associated. **(E)** Camera lucida drawing of the setae in pairs with insertion sockets associated. Ca, carapace; other abbreviations as in Figure 1. Scale bars: 2cm. Images and drawing credit: G. Potin.

MGL 103027a/b is a fragment of curved endite with setae showing length irregularities due to the incomplete preservation. It is bearing setae in pairs with clear triangular insertions.

MGL 103603a/b (Figure 8H) consist of a small fragmented endite with the inner margin bear setae, in pairs, with a regular size.

Remark: The major difference compared to *Pseudoangustidontus duplospineus* is that the setae all have the same length. There is no size alternance between even and odd setae, as seen in *Pseudoangustidontus izdigua*. MGL 104052_1 is the first *Pseudoangustidontus* that shows podomeres and confirms that the genus belongs to Radiodonta and the

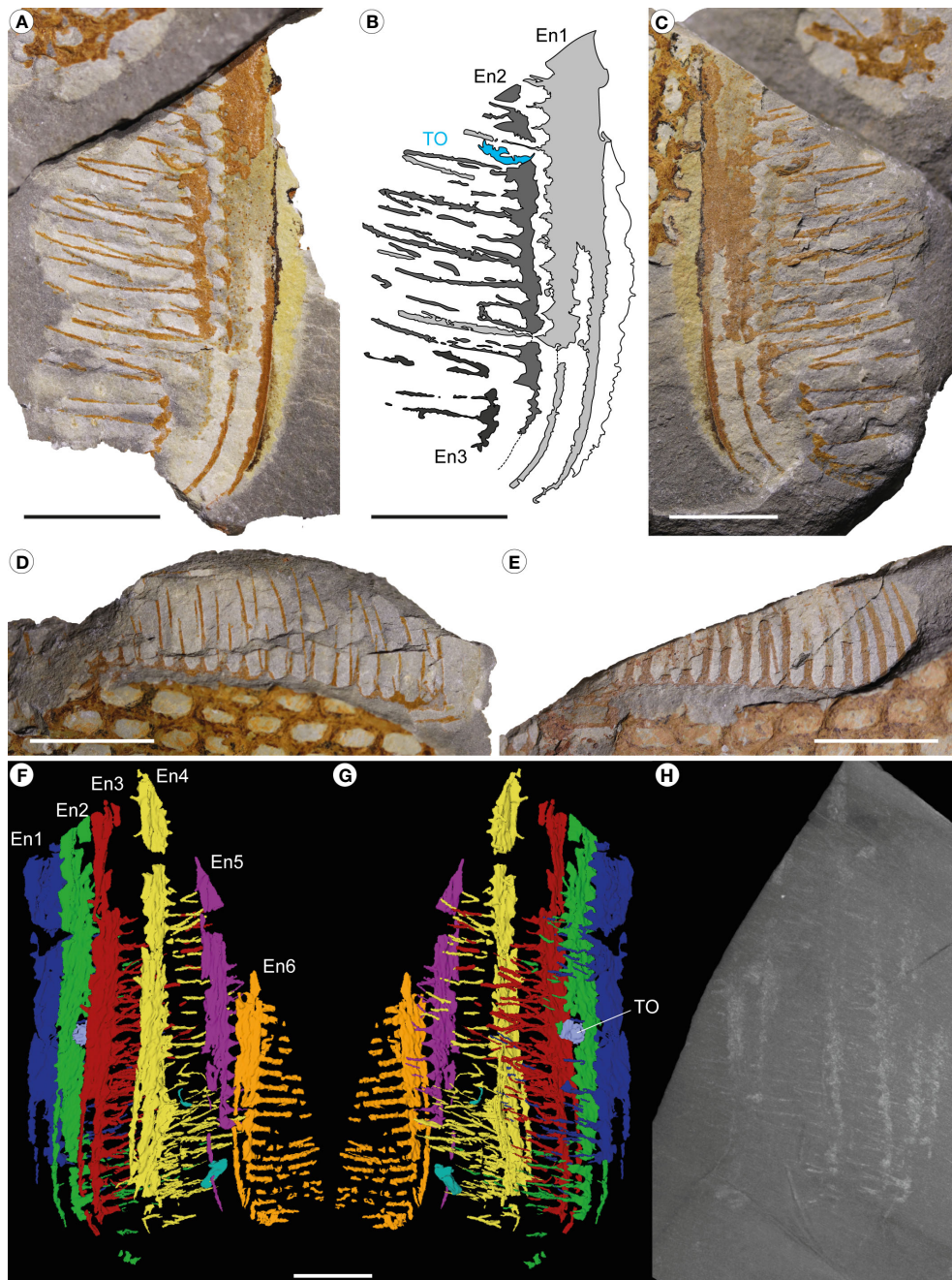


FIGURE 7

Pseudoangustidontus izdigua, MGL 103606 (paratype) from the Fezouata Shale Formation, *Sagenograptus murrayi* biozone, Morocco. (A–C) Intermediate region endites 1 to 3 showing setae in pairs and a trapped shelly prey. (A, C) Picture under polarized filter. (B) Camera lucida drawing. (D) Intermediate region endite 5 showing setae in pairs, and the setae of the 4th endite. (E) Intermediate region endite 6 showing setae. (F–H) X-ray computed microtomography. (F) 3D rendering of endites 1–6 in left lateral view. (G) 3D rendering in right lateral view. (H) Max intensity projection of 100 tomograms. TO, trapped organism; other abbreviations as in Figure 1. Scale bars: 1cm. Images and drawing credit: (A–G) G. Potin, (H) P. Gueriau.

Hurdiidae family. Sockets are visible in this species, but have not yet been observed in *P. duplospineus*.

Pseudoangustidontus sp.

Additional material MGL 102323, MGL 102326, MGL 103623_1, MGL 103624, MGL 103632, MGL 103637, MGL 107951, MGL 108052, YPM IP 517619.

Locality: Specimens collected from outcrops in the Ternata plain, c. 18 km NW of the city of Zagora (Morocco) and c. 6 km NNE of the village of Beni Zouli. GPS coordinates are curated with specimens.

Horizon: Lower Fezouata Shale, Late Tremadocian, *Sagenograptus murrayi* biozone.

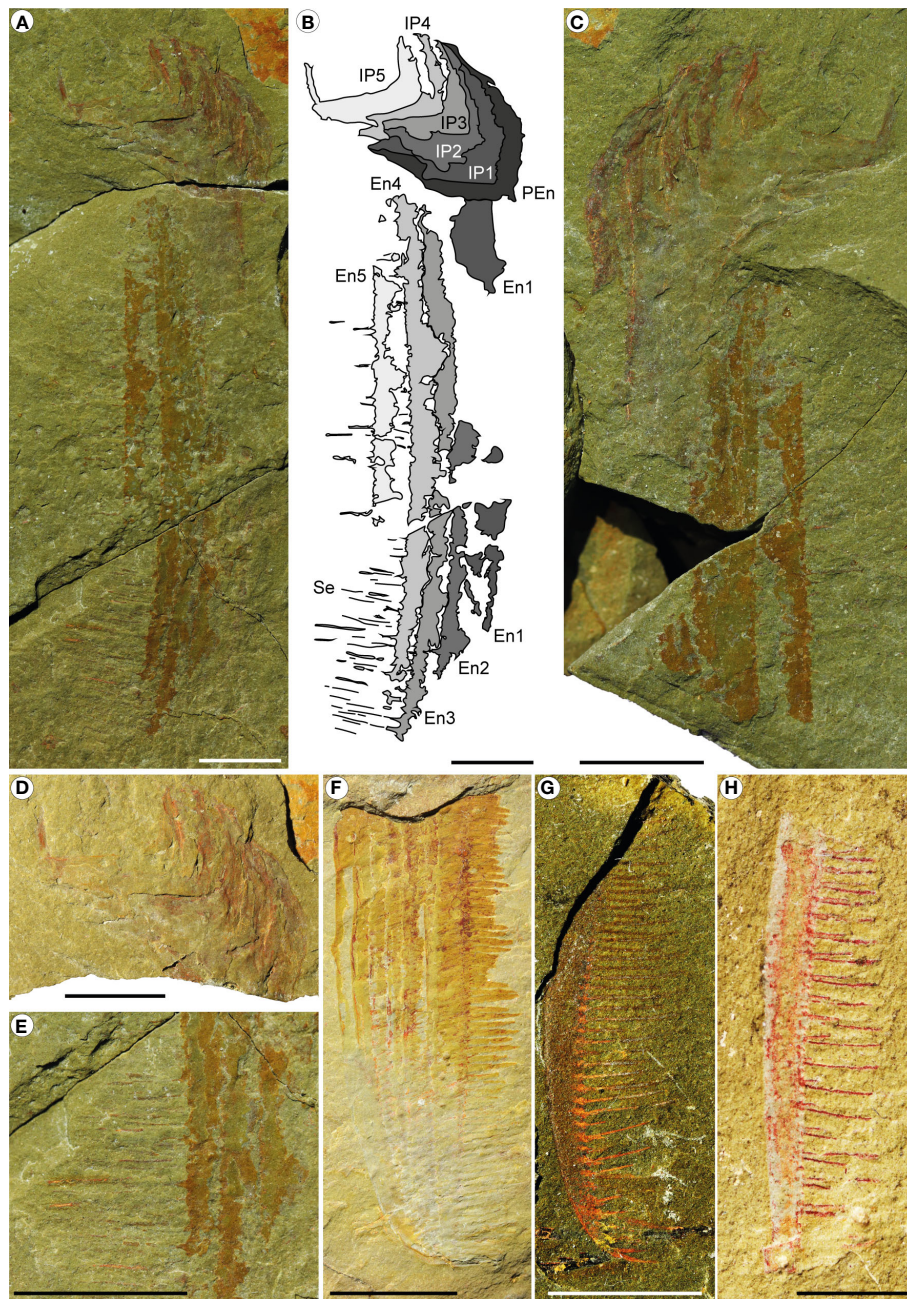


FIGURE 8

Pseudoangustidontus izdigua, from the Fezouata Shale Formation, *Sagenograptus murrayi* biozone, Morocco. (A–E) MGL 104052_1 (paratype). (A, B) Part with a series of 6 podomeres, probably the shaft podomere from the proximal region and the intermediate region podomeres 1 to 5, with the intermediate region endites 1 to 5, some with setae in pairs. (A) Picture under polarized filter. (B) Camera lucida drawing. (C) Counterpart. (D) Picture under polarized filter with a focus on the part podomeres. (E) Picture under polarized filter with a focus on the lower part of the endites and the setae in pairs. (F) YPM IP 226559 (paratype), picture under polarized filter with the 6 intermediate region endites showing setae. (G) MGL 103611, picture under polarized filter of the tip of a single intermediate region endite (one of the 5th firsts) showing setae in pairs. (H) MGL 103603 picture under polarized filter a single intermediate region endite (one of the 5th firsts) showing setae in pairs. Scale bars: (A–F): 1cm; (G, H): 0.5cm. Images and drawings credit: G. Potin.

Description: The specimens consist of endite(s) on which setae in pairs are attached, but the preservation does not allow us to distinguish if the setae size is alternating or regular.

Comments: The lack of well-preserved setae prevents identification to the species level, but they have morphological features that allow them to be identified as *Pseudoangustidontus*.

AEGIROCASSISINAE indet.

Additional material: MGL 102328, MGL 103617, MGL 103638, MGL 103651, MGL 103936_1, MGL 104062, MGL 104377, MGL 107468, MGL 108047_3, MGL 108050, MGL 108051, MGL 108055, MGL 108057, MGL 108060, YPM IP 530361.

Locality: Specimens collected from outcrops in the Ternata plain, c. 18 km NW of the city of Zagora (Morocco) and c. 6 km NNE of the village of Beni Zouli. GPS coordinates are curated with specimens.

Description: The specimens consist of endite(s) associated with setae. The preservation does not allow us to distinguish if the setae are in pairs, or if they have spinules.

Comments: The absence of well-preserved setae does not allow us to identify them to a genus level, but enough to identify the clade and therefore their feeding strategy.

6 Discussion

6.1 Implications for Systematic Paleontology

The family Hurdiidae, first mentioned by Vinther et al. (2014) and first formally described and defined by Lerosey-Aubril and Pates (2018), is characterized by possessing five podomeres each bearing at least one long endite. However, some specimens belonging to the Aegirocassisinae show six long endites, *Cordaticaris* has at least eight long endites (Sun et al., 2020a), and *Buccaspinea* has six endites with twelve podomeres (Pates et al., 2021b). Therefore, there are now several species in the Hurdiidae that have more than five long endites in the intermediate region.

Within Aegirocassisinae, a proximal region podomere with endite has only been observed in *Aegirocassis* so far (YPM IP 527125; MGL 103593; MGL 103594), so we did not include this character in the diagnosis of the broader group. Proximal region podomeres and endites are sometimes present in other Hurdiidae, e.g. *Hurdia* and questionably *Pahvantia* (Daley et al., 2013a; Lerosey-Aubril and Pates, 2018; Caron and Moysiuk, 2021), so this endite on the proximal podomere may be a character for all Hurdiidae.

Van Roy and Tetlie (2006) could not confidently place the genus *Pseudoangustidontus* in a stable phylogenetic position within Arthropoda owing to a lack of characters. *Pseudoangustidontus duplospineus* shares similarities and was named after the genus *Angustidontus* Cooper, 1936, an abundant and widespread Late Devonian fossil with enigmatic affinities at the time, but later recognized as a crustacean (Rolfe and Dzik, 2006) likely related to decapods (Gueriau et al., 2014). Van Roy and Tetlie (2006) also suggested that *Pseudoangustidontus duplospineus* could be a radiodont based upon morphological resemblance to *Echidnacaris briggsi* (Van Roy and Tetlie, 2006). With the discovery and description of *Pseudoangustidontus izdigua* sp. nov. herein, the genus can definitively be attributed to hurdiid radiodonts. Evidence comes mainly from two specimens that are sufficiently complete to demonstrate that *Pseudoangustidontus* is a radiodont. Specimen MGL 104052_1 preserves five aligned and overlapping *Pseudoangustidontus*-like “appendage fragments” in close association with six podomeres (Figures 8A–E), undoubtedly identifying them as the endites of a radiodont frontal appendage. Another specimen, MGL 103606 (Figure 7), shows a set of associated endites, aligned in parallel in the same plane but without podomeres, which are blade-like and indicate a Hurdiidae affinity. Most of the others fossils of *Pseudoangustidontus* consist of a single endite fragment with setae, suggesting a high degree of taphonomic disarticulation

before preservation. This study allows for *Pseudoangustidontus duplospineus* and *Pseudoangustidontus izdigua* sp. nov. to be assigned to the order Radiodonta and the family Hurdiidae.

The new subfamily clade Aegirocassisinae within the family Hurdiidae has been erected due to the strong similarities between *Pseudoangustidontus* and *Aegirocassis*, with both genera having long endites bearing numerous, closely spaced, thin setae that are well adapted for suspension feeding (Figure 9). The erection of the new subfamily allows for the separation of the suspension-feeding versus the non-suspension-feeding Hurdiidae, at least within the Fezouata Shale. The only other possible suspension-feeding hurdiids, *Pahvantia* (as interpreted by Lerosey-Aubril and Pates, 2018), and *Cambroraster* (as interpreted in De Vivo et al., 2021) cannot be placed in Aegirocassisinae because of the lower number of endites, the absence of a distal dimorphic endite, and presence of at least two differentiated proximal endites. Note, however, that this purported suspension-feeding frontal appendage originally described for *Pahvantia* (Lerosey-Aubril and Pates, 2018) has since been re-interpreted as setal blades, with the appendage being re-described as having robust and distantly space auxiliary spines on the endites (Caron and Moysiuk, 2021), meaning it may actually be a sediment-sifter. *Pahvantia* can therefore be excluded from the subfamily Aegirocassisinae. As far as *Cambroraster* is concerned, De Vivo et al. (2021) consider as a suspension-feeder while Caron and Moysiuk (2021) interpret this taxon as a macrophagous sediment-sifter.

Owing to its consistent placement in the Tamisiocarididae family, the other suspension-feeder *Tamisiocaris* cannot be placed in the Aegirocassisinae (Vinther et al., 2014; Paterson et al., 2023; Potin and Daley, 2023). This is also the case for the debated *Echidnacaris briggsi*, which is also placed in the Tamisiocarididae family (Vinther et al., 2014; Paterson et al., 2023; Potin and Daley, 2023). *E. briggsi* is a debated specimen concerning the feeding strategy, with Paterson et al. (2020) having interpreted it as a suspension-feeder and Caron and Moysiuk (2021) considering the feeding ecology as unknown.

6.2 Ecology

Radiodonts are a group with a large diversity of feeding ecologies, as indicated by the morphology of their frontal appendages (Collins, 1996; Daley and Budd, 2010; Lerosey-Aubril and Pates, 2018; Guo et al., 2019; Caron and Moysiuk, 2021; Potin and Daley, 2023). Some, including *Amplectobelua* and *Anomalocaris*, are active raptorial predators, and have well-articulated appendages characterised by a large number of podomeres with short endites used to catch soft and lightly sclerotised prey (Daley and Budd, 2010; Guo et al., 2019; Caron and Moysiuk, 2021; Potin and Daley, 2023). The others are filter-feeders, as can be identified by their appendage having a smaller number of podomeres bearing long, usually straight and parallel endites with auxiliary spines (Daley and Budd, 2010; Caron and Moysiuk, 2021). The latter can be divided in two subgroups: the sediment-sifters and the suspension-feeders that can be differentiated by the robustness of the auxiliary structures on the endites, the interspace between them, and the length of the endites (Caron and

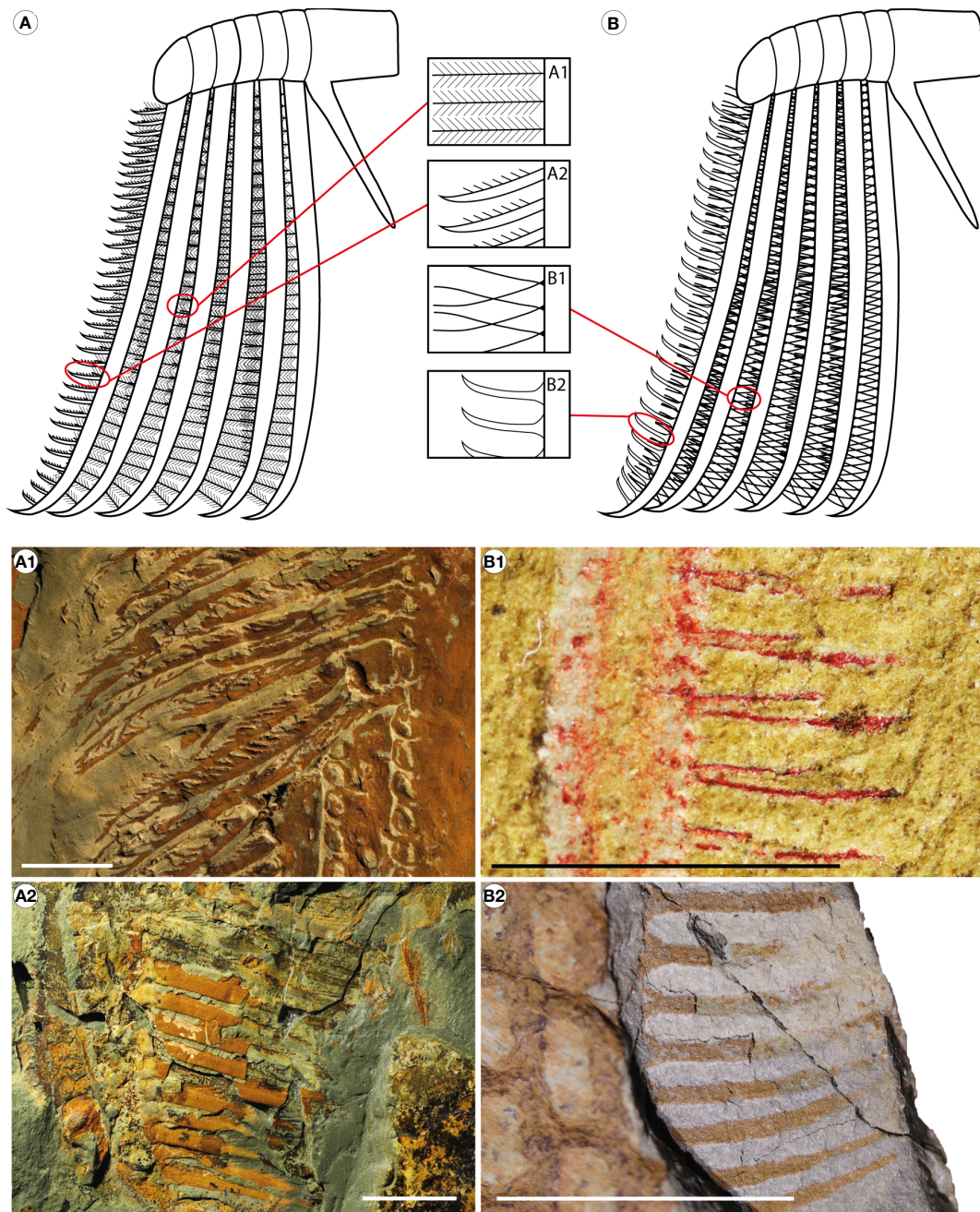


FIGURE 9

Reconstructions of Aegirocassisinae appendages with close-ups of the different setae morphologies. (A) *Aegirocassis benmoulai*. (B) *Pseudoangustidontus izdigua*. (A1) YPM IP 517125, *A. benmoulai* setae from intermediate region endites 1 to 5. (A2) YPM IP 523428, *A. benmoulai* setae from intermediate region endite 6. (B1) MGL 103603, *P. izdigua* setae from intermediate region endites 1 to 5. (B2) MGL 103606, *P. izdigua* setae from intermediate region endite 6. Scale bars: (A1, A2, B2): 1cm; (B1): 0.5cm. Images and drawings credit: (A, B, A2, B1, B2) G. Potin, (A1) A. Daley.

Moysiuk, 2021). For suspension-feeding radiodonts, auxiliary structures are called setae, because they are long and thin with a small interspace between them, and they can bear spinules (Caron and Moysiuk, 2021). The sediment sifter appendages have endites bearing auxiliary spines that are shorter and more robust with a wider interspace between them, forming a coarse, resistant mesh for sifting through sediment for infaunal prey. Endites are usually shorter in sediment-sifters as compared to suspension-feeders, to facilitate

movement through the sediment and resist breakage (Caron and Moysiuk, 2021).

In the Fezouata Shale, radiodont frontal appendages have not yet been found fully articulated with all other body parts of the animal in place, but they have been found together in disarticulated assemblages with cephalic carapaces. The position and the role of the appendages in relation to the oral cone (mouthpart) remains unknown. Nonetheless, two hypotheses have been proposed

regarding food intake mechanics in suspension-feeders. First, if the appendages were positioned directly in front of the mouth, the fine mesh created by setae and spinules would play a passive role in feeding by letting particles pass through the appendages to directly enter the oral cone. In this case, the particles captured by the setae are not consumed and are later evacuated in the water. The second hypothesis proposes that the appendages are held out anterior to the head where they play an active role in feeding by capturing what will be eaten. The small particles that pass through the setae are not consumed, and the larger plankton caught in the mesh of the frontal appendages is moved to the oral cone for consumption. This is the hypothesis that has been proposed for the function of suspension-feeding in radiodonts so far (Vinther et al., 2014; Van Roy et al., 2015b; Lerosey-Aubril and Pates, 2018), and is followed in the present work. Consequently, measuring the appendage mesh size allows for an estimation of the minimum prey size that suspension-feeding animals can capture (Sieburth et al., 1978; Vinther et al., 2014; Van Roy et al., 2015b; Lerosey-Aubril and Pates, 2018).

Previously, among suspension-feeding radiodonts, mesh sizes in *Aegirocassis benmoulai* and *Tamisiocaris* have been estimated to ca. 0.5mm in average, enabling them to capture prey of about 1 mm (Figure 10) (Vinther et al., 2014; Lerosey-Aubril and Pates, 2018). With current alignment of prey and non-spheroidal prey shape, it is estimated that the maximum length of the prey that can be ingested is around three times the mesh width (see a similar calculation for Archaeocyathan filtration in Antcliffe et al. (2019)). With the study of the new specimens, the average mesh size of *Aegirocassis benmoulai* is here re-evaluated to be 0.56mm.

The average mesh size in *Pseudoangustidontus* is ca. 0.50mm, with 0.49mm and 0.51mm in *P. duplospineus* and *P. izdigua* sp. nov., respectively. The prey of these two genera fall into the category of mesoplankton (0.2-20mm), which consists of metazooplankton (small invertebrates) and some phytoplankton and protozooplankton (Sieburth et al., 1978; Vinther et al., 2014; Lerosey-Aubril and Pates, 2018; Antcliffe et al., 2019). Early Paleozoic metazooplankton was composed of trilobitomorpha (mostly larvae), ostracods, bradoriids, copepods, malacostracan and branchiopod arthropods, as well as graptolites and chitinozoans (Perrier et al., 2015; Servais et al., 2016). For the possible suspension-feeder *Pahvantia*, the mean mesh size was measured to be 0.7mm, which allowed it to capture smaller (>0.10mm) prey (Figure 10) (Lerosey-Aubril and Pates, 2018), including large microplankton (mainly phytoplankton and protozooplankton) and the smallest mesoplankton (Sieburth et al., 1978; Vinther et al., 2014; Lerosey-Aubril and Pates, 2018), which in the Early Paleozoic could include eggs, arthropod larvae and small specimens of acritarchs or chitinozoans (Perrier et al., 2015; Servais et al., 2016).

In the paratype of *Pseudoangustidontus izdigua* sp. nov. (MGL 103606), a unidentified shell or carapace is trapped by the setae of endites 4 and 5 (see Figure 7, abbreviated TO). The size of this carapace (ca. 3 mm in diameter) is larger than the size of the prey that has been estimated for this species (Figure 10). The presence of this captured prey highlights the fact that mesh size only provides an estimation of the minimum potential prey size. Such estimations have been made based on average values from extant organisms, so

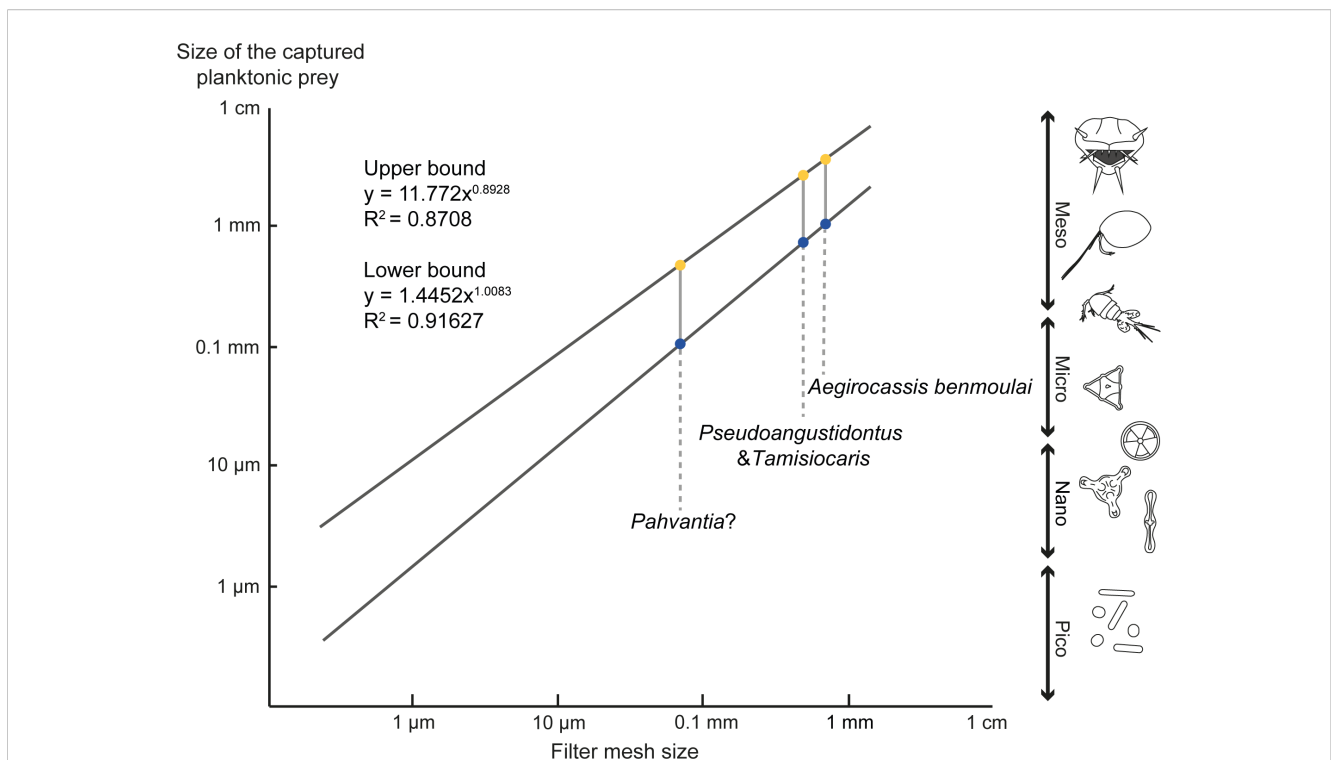


FIGURE 10 Size of captured particles by the suspension-feeding radiodonts. Data have been compiled from Vinther et al. (2014); Van Roy et al. (2015b) and Lerosey-Aubril and Pates (2018), and the graph modified from Vinther et al. (2014).

the range of the prey size can be larger than this average (Vinther et al., 2014).

The identification in this study of dimorphism in the appendages of *Aegirocassis* indicates that food intake was even more complex than previously described. The larger mesh size of the dimorphic endite (En6) has not been taken into account in calculations of estimated prey size because it has a coarser mesh size and would therefore not contribute to the minimum prey size estimation. Given that endite 6 is the most distal endite, it could have had a role as a coarse first filter, capturing large particles that would otherwise have the potential to damage the five other endites with their fine setae and spinules, and therefore had a protection role. It may also have had a strengthening role, acting as a more robust framework or scaffold to lend stability to the whole endite-bearing region of the frontal appendage. Additionally, if angled towards the mouth, it could have funnelled particles onto the other endites.

6.3 Diversity of suspension-feeding radiodonts

Only three suspension-feeding radiodonts had been described previously: *Aegirocassis*, *Tamisiocaris* and questionably *Pahvantia* (Vinther et al., 2014; Van Roy et al., 2015b; Lerosey-Aubril and Pates, 2018; Pates and Daley, 2019; Pates et al., 2019; Caron and Moysiuk, 2021). *Pseudoangustidontus* is herein described as the fourth genus of suspension-feeding radiodont. As the new subfamily

Aegirocassinae contains three species (*Aegirocassis benmoulai*, *Pseudoangustidontus duplospineus* and *Pseudoangustidontus izdigua* sp. nov.), the Ordovician Fezouata Shale is the locality with the highest known species diversity of suspension-feeding radiodonts, making the Tremadocian stage the most diverse time for suspension-feeding radiodonts (Figure 11). The only definitive suspension-feeding radiodont taxon described from the Cambrian is *Tamisiocaris borealis* Daley and Peel, 2010 and questionably *Pahvantia hastata* Robison and Richards, 1981, *Cambroraster falcatus* Moysiuk and Caron, 2019 and *Echidnacaris briggsi* Nedin, 1995 (Robison and Richards, 1981; Nedin, 1995; Daley and Peel, 2010; Daley et al., 2013b; Vinther et al., 2014; Lerosey-Aubril and Pates, 2018; Moysiuk and Caron, 2019; Pates and Daley, 2019; Pates et al., 2019; Potin and Daley, 2023; Paterson et al., 2023).

Tamisiocaris, the only definitive Cambrian suspension-feeding radiodont was found in the Cambrian Stage 3 and Stage 4 Kinzers Formation in Pennsylvania, and also in the Cambrian Series 2 Stage 3 Sirius Passet Formation in Greenland (Figure 11) (Daley and Peel, 2010; Vinther et al., 2014; Lerosey-Aubril and Pates, 2018; Pates and Daley, 2019; Pates et al., 2019). *Cambroraster* is also found in the Cambrian Stage 4 of the Chengjiang Biota (China), and in the Wuliuan at the Burgess Shale (Canada) and the Mantou Formation (China) (Moysiuk and Caron, 2019; Liu et al., 2020; Sun et al., 2020b; Paterson et al., 2023; Potin and Daley, 2023). *Echidnacaris briggsi* is exclusively found in the Emu Bay Shale in Australia, dated from the Cambrian Stage 4 (Daley et al., 2013b; Potin and Daley, 2023; Paterson et al., 2023). *Pahvantia* was reported from the Lower Drumian (middle Cambrian) Wheeler and Marjum Formations in Utah (Figure 11)

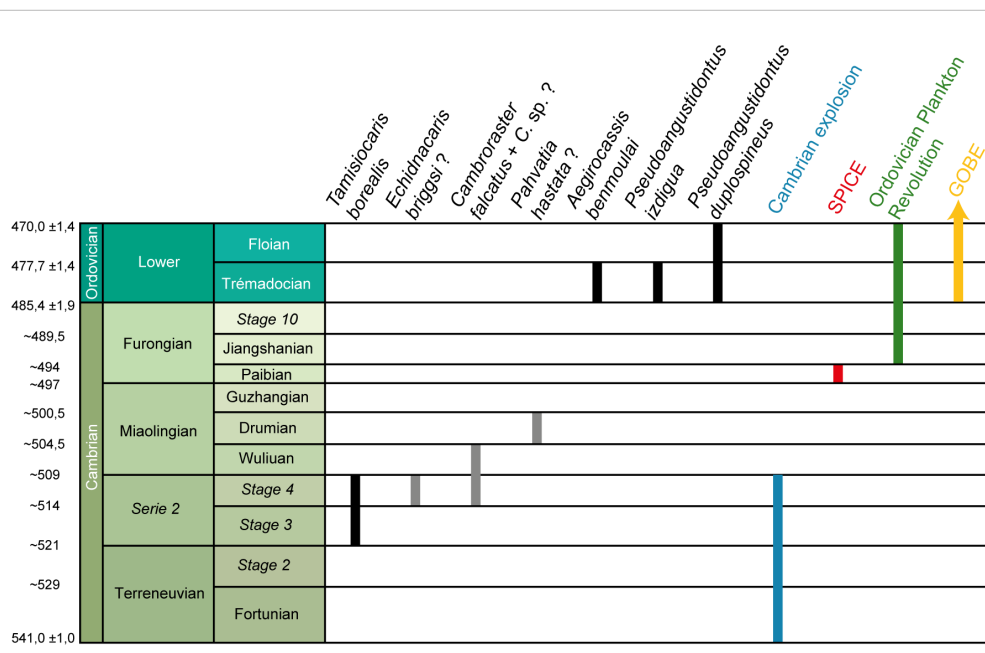


FIGURE 11 Stratigraphic distribution of suspension-feeding radiodonts species and major evolutionary events during the early Paleozoic. Grey bars represent taxa where suspension-feeding interpretations are debated. Data have been compiled from Robison and Richards (1981); Nedin (1995); Van Roy and Tettie (2006); Daley and Budd (2010); Saltzman et al. (2011); Daley et al. (2013b); Vinther et al. (2014); Servais et al. (2016); Vaucher et al. (2016); Lerosey-Aubril and Pates (2018); Moysiuk and Caron (2019); Paterson et al. (2019); Pates and Daley (2019); Pates et al. (2019); Liu et al. (2020); Sun et al. (2020b). Modified from Cohen et al. (2013).

(Robison and Richards, 1981; Lerosey-Aubril and Pates, 2018; Pates et al., 2019; Pates et al., 2021b; Potin and Daley, 2023).

Tamisiocaris is not a hurdiid radiodont and has an appendage morphology characterised by having at least 18 podomeres each bearing a pair of long endites with densely packed setae (Daley and Peel, 2010; Vinther et al., 2014). In phylogenetic analyses, it typically forms a clade with *Echidnacaris briggsi*, which some authors has considered to be a suspension-feeder (Vinther et al., 2014; Paterson et al., 2020), though this ecological interpretation has been challenged (Daley et al., 2013b). The clade of these two taxa does not have a stable position in the radiodont phylogenetic tree, and has been retrieved as sister group to all other radiodont families depending on the matrix coding and methods used (e.g. see figure 8 in Potin and Daley, 2023). In all cases, it has never been retrieved together with *Aegirocassis* and so can be considered as a separate evolutionary innovation of suspension feeding that was restricted to the Cambrian and was not associated with a large body size.

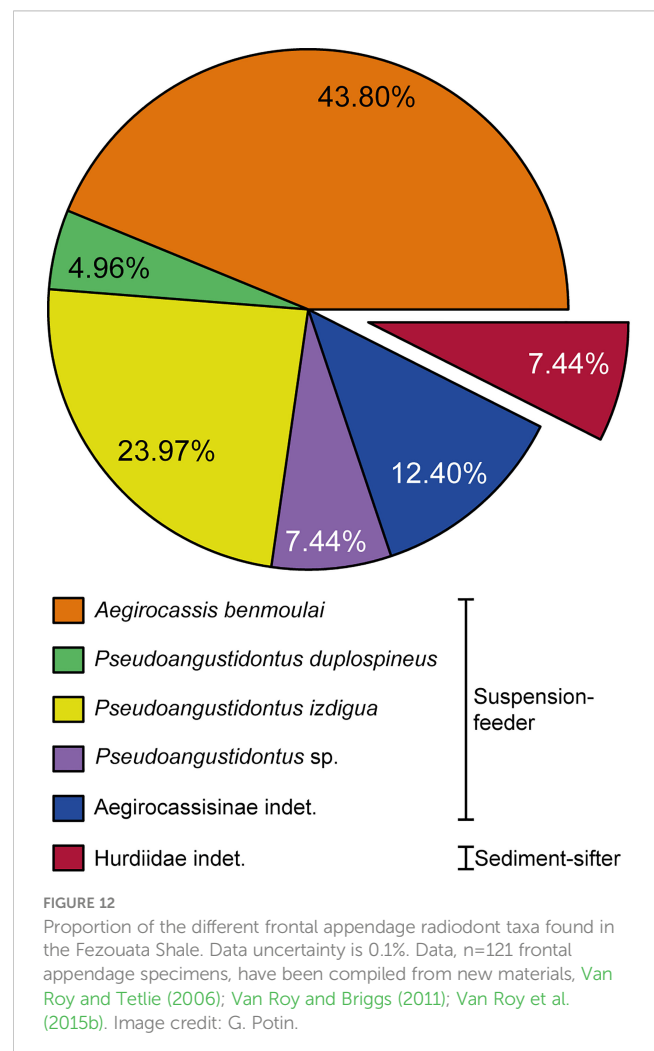
6.4 Dominance of suspension-feeding radiodonts during the GOBE

In the Fezouata Shale collections examined in this study, suspension-feeding frontal appendages are dominant in terms of proportion among the studied specimens, with only eight out of 105 total known hurdiid appendages indicating a sediment-sifting mode of feeding rather than suspensions feeding (Figure 12). Two of these sediment-sifter frontal appendages (YPM 227644 and YPM 227646) have been reported in Van Roy and Briggs (2011), to which we add a further six from this study. Outside the Fezouata Biota, another Early Ordovician hurdiid appendage (NMW 2012.36G.90) from the Tremadocian Afon Gam Biota (Dol-cyn-Afon Formation) in Wales (Pates et al., 2020) shares anatomical similarities with sediment-sifter radiodonts rather than suspensions feeding radiodonts.

The strong dominance of suspension-feeding over sediment-sifting radiodonts in the Fezouata Shale, as well as the overall higher diversity of suspension-feeders during the Ordovician, could be related to the “Ordovician Plankton Revolution” that took place during the Upper Cambrian and Lower Ordovician (Servais et al., 2010; Servais et al., 2016). This event saw the rapid diversification of plankton within many groups such as acritarchs, graptolites, chitinozoans, radiolarians but also small planktonic arthropods (such as pelagic trilobites and phyllocarid crustaceans) and cephalopods (Servais et al., 2016). Although the origin(s) of the Ordovician Plankton Revolution remain extensively debated, it appears to be related to the “Steptoean Positive Carbon Isotope Excursion $\delta^{13}C_{carb}$ ” (SPICE) that took place during the Paibian (Furogian) (Servais et al., 2016). The SPICE is associated with an increase in atmospheric oxygen as well as an increase in nutrients available in the oceans (Servais et al., 2016). The Ordovician Plankton Revolution completely modified the structures of food chains allowing the diversification and abundance of suspension-feeding organisms during the early part of the Ordovician period (Servais et al., 2010; Van Roy et al., 2015b; Servais et al., 2016). Thus, the greater diversity of plankton may have incited diversification in suspension-feeding organisms, resulting in increased morphological

diversity of radiodonts with frontal appendages specialised for feeding in the early Ordovician Fezouata Shale.

On the other hand, the associated decline in raptorial predator radiodonts is also estimated to have taken place around the early Ordovician period. This decline could be explained by an increase in competition with other predators such as cephalopods (Pates et al., 2020), which probably appeared during the early Cambrian (Hildenbrand et al., 2021) and were the top predators in the food chain during the Ordovician (Kröger and Zhang, 2009; Kröger et al., 2009). Cephalopods underwent a rapid diversification during the Ordovician radiation particularly in the pelagic domain during the Tremadocian (Kröger et al., 2009). The presence of cephalopods in the Ordovician of the Fezouata Shale is well known (Van Roy et al., 2010; Kröger and Lefebvre, 2012; Van Roy et al., 2015a). The competition between cephalopods and anomalocaridids may have been to the advantage of the cephalopods owing to their better adaptation and efficiency in swimming and thus predation (Klug et al., 2010; Whalen and Briggs, 2018). The emergence of other predatory taxa such as eurypterids, whose presence has been documented in the Fezouata Shale based on a few fragmentary remains (Van Roy et al., 2015a); note that this would predates the earliest-known, Darriwilian, eurypterids, Lamsdell et al. (2015) may have accentuated the decline of raptorial predator radiodonts.



7 Conclusion

The study of new specimens and new species of radiodonts from the Fezouata Shale Formation has clarified the diversity and ecology of Hurdiidae at this locality, and allowed for the erection of a new subfamily Aegirocassisinae. This new subfamily includes two species of *Pseudoangustidontus* and *Aegirocassis benmoulai*. The presence of dimorphic endites bearing long-thin setae in these taxa is particularly distinctive. This group contains all the suspension-feeding radiodonts from the Fezouata Shale. During the Lower Ordovician suspension-feeding radiodonts are the dominant form of the group, following the “Ordovician Plankton Revolution” that saw a major radiation in plankton diversity. Measurements of the mesh size of the different frontal appendages within Aegirocassisinae allowed us to estimate the size of the preys that they could have captured, revealing that they mostly ate mesoplankton. Finally, only two feeding strategies have been identified among Fezouata radiodonts: suspension-feeding and sediment sifting. We found, however, no evidence for any active apex predator similar to *Anomalocaris*, while they were common during the Cambrian. This highlights the high competition with other large active nektonic predators that rapidly evolved during the Lower Ordovician, such as cephalopods or eurypterid arthropods. As a result, the evolutionary and ecological plasticity of the radiodonts can be seen as they adapt to a rapidly changing Ordovician world.

Data availability statement

The original contributions presented in the study are included in the article/Supplementary Material. Further inquiries can be directed to the corresponding author.

Author contributions

AD and GP designed the project, and GP examined, photographed and drew the fossil material. Advanced imaging and analytical techniques were performed by PG and GP. Fossil interpretations were done together with all authors, who also all contributed to writing the manuscript. GP prepared the figures and Supplementary Material.

Funding

GP and this research were funded by the Canton de Vaud and the Swiss National Science Foundation, grant number 205321_179084 entitled “Arthropod Evolution during the Ordovician Radiation: Insights from the Fezouata Biota” and awarded to AD.

Acknowledgments

We are grateful to Lukáš Laibl (Czech Academy of Sciences), Susan Butts (Yale Peabody Museum) and Jessica Utrup (Yale Peabody Museum), Bertrand Lefebvre (University Claude Bernard Lyon 1) for access to the material from the collection of the University of Lausanne, the Yale Peabody Museum and the Marrakech Collections of the Cadi Ayyad University (stored in University Claude Bernard Lyon 1) respectively. Benita Putlitz (UNIL) ran μ CT scanning, and Julien Alleon (UNIL) provided assistance with Raman microspectroscopy. We thank Jonathan B. Antcliff (UNIL) for English language editing of the manuscript. We acknowledge the SOLEIL Synchrotron for provision of beamtime, and Cristian Mocuta, Dominique Thiaudière, Solenn Réguer and Philippe Joly (SOLEIL Synchrotron) for assistance at the DiffAbs beamline. We thank Pénélope Claisse, Lorenzo Lustri, Sinéad Lynch and Francesc Pérez-Peris (UNIL) for their help with the statistical analysis, Farid Saleh (Yunnan University) for discussion about taphonomy and preservation in the Fezouata Shale, and Peter Van Roy for discussion about Fezouata radiodonts. We thank Ismail Khardali for the translation of the word “filter” in Tamazight language used to name the new species of *Pseudoangustidontus*.

Conflict of interest

The authors declare that the research was conducted in the absence of any commercial or financial relationships that could be construed as a potential conflict of interest.

Publisher’s note

All claims expressed in this article are solely those of the authors and do not necessarily represent those of their affiliated organizations, or those of the publisher, the editors and the reviewers. Any product that may be evaluated in this article, or claim that may be made by its manufacturer, is not guaranteed or endorsed by the publisher.

Supplementary material

The Supplementary Material for this article can be found online at: <https://www.frontiersin.org/articles/10.3389/fevo.2023.1214109/full#supplementary-material>

References

- Antcliffe, J. B., Jessop, W., and Daley, A. C. (2019). Prey fractionation in the Archaeocyatha and its implication for the ecology of the first animal reef systems. *Paleobiology* 45 (4), 652–675. doi: 10.1017/pab.2019.32
- Briggs, D. E. G. (1979). *Anomalocaris*, the largest known Cambrian arthropod. *Palaentology* 22 (3), 631–664.
- Caron, J.-B., Gaines, R. R., Mángano, M. G., Streng, M., and Daley, A. C. (2010). A new Burgess Shale-type assemblage from the “thin” Stephen Formation of the southern Canadian Rockies. *Geology* 38 (9), 811–814. doi: 10.1130/G31080.1
- Caron, J.-B., and Moysiuk, J. (2021). A giant nektobenthic radiodont from the Burgess Shale and the significance of hurdiid carapace diversity. *R. Soc. Open Sci.* 8 (9), 210664. doi: 10.1098/rsos.210664
- Cohen, K. M., Finney, S. C., Gibbard, P. L., and Fan, J. -X. (2013). *The ICS International Chronostratigraphic Chart. Episodes* 36:199–204.
- Collins, D. (1996). The “evolution” of *Anomalocaris* and its classification in the arthropod class Dinocarida (nov.) and order Radiodonta (nov.). *J. Paleontol.* 70 (2), 280–293. doi: 10.1017/S002233600023362
- Cong, P. Y., Edgecombe, G. D., Daley, A. C., Guo, J., Pates, S., and Hou, X. G. (2018). New radiodonts with gnathobase-like structures from the Cambrian Chengjiang Biota and implications for the systematics of Radiodonta. *Papers Palaentol.* 4 (4), 605–621. doi: 10.1002/spp2.1219
- Conway Morris, S., and Whittington, H. B. (1979). The animals of the Burgess Shale. *Sci. Am.* 241 (1), 122–135. <https://www.jstor.org/stable/24965247>
- Cooper, C. L. (1936). Actinopterygian jaws from the Mississippian black Shale of the Mississippi valley. *J. Paleontol.* 10 (2), 92–94. <https://www.jstor.org/stable/1298344>
- Daley, A. C., and Budd, G. E. (2010). New anomalocaridid appendages from the Burgess Shale, Canada. *Palaentology* 53 (4), 721–738. doi: 10.1111/j.1475-4983.2010.00955.x
- Daley, A. C., Budd, G. E., and Caron, J.-B. (2013a). Morphology and systematics of the anomalocaridid arthropod *Hurdia* from the middle Cambrian of British Columbia and Utah. *J. Syst. Palaentol.* 11 (7), 743–787. doi: 10.1080/14772019.2012.732723
- Daley, A. C., Paterson, J. R., Edgecombe, G. D., García-Bellido, D. C., and Jago, J. B. (2013b). New anatomical information on *Anomalocaris* from the Cambrian Emu Bay Shale of South Australia and a reassessment of its inferred predatory habits. *Palaentology* 56 (5), 971–990. doi: 10.1111/pala.12029
- Daley, A. C., and Peel, J. S. (2010). A possible anomalocaridid from the Cambrian Sirius Passet Lagerstätten, North Greenland. *J. Paleontol.* 84 (2), 352–355. doi: 10.1666/09-136R1.1
- De Vivo, G., Lautenschlager, S., and Vinther, J. (2021). Three-dimensional modelling, disparity and ecology of the first Cambrian apex predators. *Proc. R. Soc. B* 288, 20211176. doi: 10.1098/rspb.2021.1176
- Drage, H. B., Vandenbroucke, T. R. A., Van Roy, P., and Daley, A. C. (2019). Sequence of post-moult exoskeleton hardening preserved in a trilobite mass moult assemblage from the Lower Ordovician Fezouata Konservat-Lagerstätte, Morocco. *Acta Palaentologica Polonica* 64 (2), 261–273. doi: 10.4202/app.00582.2018
- Gaines, R. R., Briggs, D. E. G., Orr, P. J., and Van Roy, P. (2012). Preservation of giant anomalocaridids in silica-chlorite concretions from the Early Ordovician of Morocco. *Palaos* 27 (5), 317–325. doi: 10.2110/palo.2011.p11-093r
- Guerau, P., Charbonnier, S., and Clément, G. (2014). Angustidontid crustaceans from the Late Devonian of Strud (Namur Province, Belgium): insights into the origin of Decapoda. *Neues Jahrbuch für Geologie und Paläontologie* 273 (3), 327–337. doi: 10.1127/0077-7749/2014/0434
- Guo, J., Pates, S., Cong, P., Daley, A. C., Edgecombe, G. D., Chen, T., et al. (2019). A new radiodont (stem Euarthropoda) frontal appendage with a mosaic of characters from the Cambrian (Series 2 Stage 3) Chengjiang Biota. *Papers Palaentol* 5 (1), 99–110. doi: 10.1002/spp2.1231
- Gutiérrez-Marco, J. C., García-Bellido, D. C., Rábano, I., and Sá, A. A. (2017). Digestive and appendicular soft-parts, with behavioural implications, in a large Ordovician trilobite from the Fezouata Lagerstätten, Morocco. *Sci. Rep.* 7 (1), 39728. doi: 10.1038/srep39728
- Hammer, Ø., and Harper, D. A. T. (2008). *Palaentological data analysis* (New Jersey, USA: John Wiley & Sons).
- Hammer, Ø., Harper, D. A. T., and Ryan, P. D. (2001). Palaentological statistics software package for education and data analysis. *Palaentologia Electronica* 4 (1), 4–9.
- Hildenbrand, A., Austermann, G., Fuchs, D., Bengtson, P., and Stinnesbeck, W. (2021). A potential cephalopod from the early Cambrian of eastern Newfoundland, Canada. *Commun. Biol.* 4 (1), 388. doi: 10.1038/s42003-021-01885-w
- Klug, C., Kröger, B., Kiessling, W., Mullins, G. L., Servais, T., Frýda, J., et al. (2010). The Devonian nekton revolution. *Lethaia* 43 (4), 465–477. doi: 10.1111/j.1502-3931.2009.00206.x
- Kröger, B., and Lefebvre, B. (2012). Palaeeogeography and palaeeoecology of early Floian (Early Ordovician) cephalopods from the upper Fezouata formation, Anti-Atlas, Morocco. *Fossil Rec.* 15 (2), 61–75. doi: 10.1002/mmng.201200004
- Kröger, B., Servais, T., and Zhang, Y. (2009). The origin and initial rise of pelagic cephalopods in the Ordovician. *PLoS One* 4 (9), e7262. doi: 10.1371/journal.pone.0007262
- Kröger, B., and Zhang, Y.-D. (2009). Pulsed cephalopod diversification during the Ordovician. *Palaeeogeogr. Palaeeoclimatol. Palaeeoecol.* 273 (1-2), 174–183. doi: 10.1016/j.palaeeo.2008.12.015
- Kühl, G., Briggs, D. E. G., and Rust, J. (2009). A great-appendage arthropod with a radial mouth from the Lower Devonian Hunsrück Slate, Germany. *Science* 323 (5915), 771–773. doi: 10.1126/science.1166586
- Lamsdell, J. C., Briggs, D. E. G., Liu, H. P., Witzke, B. J., and McKay, R. M. (2015). The oldest described eurypterid: a giant Middle Ordovician (Darrivillan) megalograptid from the Winneshiek Lagerstätten of Iowa. *BMC Evol. Biol.* 15 (1), 169. doi: 10.1186/s12862-015-0443-9
- Lebrun, P. (2017). Le biotope de Fezouata: un gisement fossilifère d'exception de l'Ordovicien Inférieur du Maroc. *Fossiles Rev. française paléontologie* 31, 5–30.
- Leclercq, N., Berthault, J., Langlois, F., Le, S., Poirier, S., Bisou, J., et al. (2015). “Flyscan: a fast and multi-technique data acquisition platform for the SOLEIL beamlines.” in *Proceedings of the 15th International Conference on Accelerator and Large Experimental Physics Control Systems (ICALPECS 2015)*, Melbourne, Australia, October 17–23, 2015. doi: 10.18429/JACO-W-ICALPECS2015-WEPGF056
- Lefebvre, B., Gutiérrez-Marco, J. C., Lehnert, O., Martin, E. L. O., Nowak, H., Akodad, M., et al. (2018). Age calibration of the Lower Ordovician Fezouata Lagerstätten, Morocco. *Lethaia* 51 (2), 296–311. doi: 10.1111/let.12240
- Lerosey-Aubril, R., and Pates, S. (2018). New suspension-feeding radiodont suggests evolution of microplanktivory in Cambrian macronekton. *Nat. Commun.* 9 (1), 3774. doi: 10.1038/s41467-018-06229-7
- Liu, Y., Lerosey-Aubril, R., Audo, D., Zhai, D., Mai, H., and Ortega-Hernández, J. (2020). Occurrence of the eudemeral radiodont *Cambroraster* in the early Cambrian Chengjiang Lagerstätten and the diversity of hurdiid ecomorphotypes. *Geol. Mag.* 157 (7), 1200–1206. doi: 10.1017/S0016756820000187
- Liu, J., Lerosey-Aubril, R., Steiner, M., Dunlop, J. A., Shu, D., and Paterson, J. R. (2018). Origin of raptorial feeding in juvenile euarthropods revealed by a Cambrian Radiodontan. *Natl. Sci. Rev.* 5 (6), 863–869. doi: 10.1093/nsr/nwy057
- Martin, E. L. O., Lerosey-Aubril, R., and Vannier, J. (2016a). Palaeeoscolicid worms from the Lower Ordovician Fezouata Lagerstätten, Morocco: palaeeoecological and palaeeogeographical implications. *Palaeeogeogr. Palaeeoclimatol. Palaeeoecol.* 460, 130–141. doi: 10.1016/j.palaeeo.2016.04.009
- Martin, E. L. O., Pittet, B., Gutiérrez-Marco, J.-C., Vannier, J., El Hariri, K., Lerosey-Aubril, R., et al. (2016b). The Lower Ordovician Fezouata Konservat-Lagerstätten from Morocco: age, environment and evolutionary perspectives. *Gondwana Res.* 34, 274–283. doi: 10.1016/j.gr.2015.03.009
- Martin, E. L. O., Vidal, M., Vizcaino, D., Vaucher, R., Sansjofre, P., Lefebvre, B., et al. (2016c). Biostratigraphic and palaeeoenvironmental controls on the trilobite associations from the Lower Ordovician Fezouata Shale of the central Anti-Atlas, Morocco. *Palaeeogeogr. Palaeeoclimatol. Palaeeoecol.* 460, 142–154. doi: 10.1016/j.palaeeo.2016.06.003
- Moysiuk, J., and Caron, J.-B. (2019). A new hurdiid radiodont from the Burgess Shale evinces the exploitation of Cambrian infaunal food sources. *Proc. R. Soc. B* 286 (1908), 20191079. doi: 10.1098/rspb.2019.1079
- Moysiuk, J., and Caron, J.-B. (2021). Exceptional multifunctionality in the feeding apparatus of a mid-Cambrian radiodont. *Paleobiology* 47 (4), 704–724. doi: 10.1017/pab.2021.19
- Moysiuk, J., and Caron, J.-B. (2022). A three-eyed radiodont with fossilized neuroanatomy informs the origin of the arthropod head and segmentation. *Curr. Biol.* 32 (15), 3302–3316. e3302. doi: 10.1016/j.cub.2022.06.027
- Nedin, C. (1995). The Emu Bay Shale, a lower Cambrian fossil Lagerstätten, Kangaroo Island, South Australia. *Memoirs Assoc. Australas. Palaentologists* 18, 31–40.
- Nedin, C. (1999). *Anomalocaris* predation on nonmineralized and mineralized trilobites. *Geology* 27 (11), 987–990. doi: 10.1130/0091-7613(1999)027<0987:APONAM>2.3.CO;2
- Nielsen, C. (1995). *Animal evolution: interrelationships of the living phyla* (Oxford, United Kingdom, Oxford University Press).
- Ortega-Hernández, J., Van Roy, P., and Lerosey-Aubril, R. (2016). A new aglaspoid euarthropod with a six-segmented trunk from the Lower Ordovician Fezouata Konservat-Lagerstätten, Morocco. *Geological Magazine* 153 (3), 524–536. doi: 10.1017/S0016756815000710
- Paterson, J. R., Edgecombe, G. D., and García-Bellido, D. C. (2020). Disparate compound eyes of Cambrian radiodonts reveal their developmental growth mode and diverse visual ecology. *Sci. Adv.* 6 (49), eabc6721. doi: 10.1126/sciadv.abc6721
- Paterson, J. R., Edgecombe, G. D., and Lee, M. S. Y. (2019). Trilobite evolutionary rates constrain the duration of the Cambrian explosion. *Proc. Natl. Acad. Sci.* 116 (10), 4394–4399. doi: 10.1073/pnas.1819366116
- Paterson, J. R., García-Bellido, D. C., and Edgecombe, G. D. (2023). The early Cambrian Emu Bay Shale radiodonts revisited: morphology and systematics. *J. Syst. Palaentol.* 21 (1), 2225066. doi: 10.1080/14772019.2023.2225066
- Pates, S., Botting, J. P., McCobb, L. M. E., and Muir, L. A. (2020). A miniature Ordovician hurdiid from Wales demonstrates the adaptability of Radiodonta. *R. Soc. Open Sci.* 7 (6), 200459. doi: 10.1098/rsos.200459

- Pates, S., and Daley, A. C. (2019). The Kinzers Formation (Pennsylvania, USA): the most diverse assemblage of Cambrian Stage 4 radiodonts. *Geological Magazine* 156 (7), 1233–1246. doi: 10.1017/S0016756818000547
- Pates, S., Daley, A. C., and Butterfield, N. J. (2019). First report of paired ventral endites in a hurdiid radiodont. *Zoological Lett.* 5 (1), 18. doi: 10.1186/s40851-019-0132-4
- Pates, S., Daley, A. C., Edgecombe, G. D., Cong, P., and Lieberman, B. S. (2021a). Systematics, preservation and biogeography of radiodonts from the Southern Great Basin, USA, during the upper Dyeran (Cambrian Series 2, Stage 4). *Papers Palaeontol.* 7 (1), 235–262. doi: 10.1002/spp2.1277
- Pates, S., Lerosey-Aubril, R., Daley, A. C., Kier, C., Bonino, E., and Ortega-Hernández, J. (2021b). The diverse radiodont fauna from the Marjum Formation of Utah, USA (Cambrian: Drumian). *PeerJ* 9, e10509. doi: 10.7717/peerj.10509
- Pérez-Peris, F., Laibl, L., Lustris, L., Gueriau, P., Antcliffe, J. B., Bath Enright, O. G., et al. (2021a). A new nektaspid euarthropod from the Lower Ordovician strata of Morocco. *Geological Magazine* 158 (3), 509–517. doi: 10.1017/S001675682000062X
- Pérez-Peris, F., Laibl, L., Vidal, M., and Daley, A. C. (2021b). Systematics, morphology, and appendages of an early Ordovician pilekiine trilobite *Anacheirurus* from Fezouata Shale and the early diversification of Cheiruridae. *Acta Palaeontologica Polonica* 66 (4), 857–877. doi: 10.4202/app.00902.2021
- Perrier, V., Williams, M., and Siveter, D. J. (2015). The fossil record and palaeoenvironmental significance of marine arthropod zooplankton. *Earth-Science Rev.* 146, 146–162. doi: 10.1016/j.earscirev.2015.02.003
- Potin, G. J.-M., and Daley, A. C. (2023). The significance of *Anomalocaris* and other Radiodonts for understanding palaeoecology and evolution during the Cambrian explosion. *Front. Earth Sci.* 11. doi: 10.3389/feart.2023.1160285
- Robison, R. A., and Richards, B. C. (1981). Larger bivalve arthropods from the middle Cambrian of Utah. *Kansas Paleontological Contributions* 106, 1–28. <https://hdl.handle.net/1808/3757>
- Rolfé, W. D. I., and Dzik, J. (2006). *Angustidontus*, a Late Devonian pelagic predatory crustacean. *Trans. R. Soc. Edinburgh: Earth Sci.* 97 (1), 75–96. doi: 10.1017/S0263593300001413
- Saleh, F., Antcliffe, J. B., Lefebvre, B., Pittet, B., Laibl, L., Pérez-Peris, F., et al. (2020a). Taphonomic bias in exceptionally preserved biotas. *Earth Planetary Sci. Lett.* 529, 115873. doi: 10.1016/j.epsl.2019.115873
- Saleh, F., Bath-Enright, O. G., Daley, A. C., Lefebvre, B., Pittet, B., Vite, A., et al. (2021a). A novel tool to untangle the ecology and fossil preservation knot in exceptionally preserved biotas. *Earth Planetary Sci. Lett.* 569, 117061. doi: 10.1016/j.epsl.2021.117061
- Saleh, F., Candela, Y., Harper, D. A. T., Polechová, M., Lefebvre, B., and Pittet, B. (2018). Storm-induced community dynamics in the Fezouata Biota (Lower Ordovician, Morocco). *Palaios* 33 (12), 535–541. doi: 10.2110/palo.2018.055
- Saleh, F., Guenser, P., Gibert, C., Balseiro, D., Serra, F., Waisfeld, B. G., et al. (2022a). Contrasting Early Ordovician assembly patterns highlight the complex initial stages of the Ordovician radiation. *Sci. Rep.* 12 (1), 3852. doi: 10.1038/s41598-022-07822-z
- Saleh, F., Lefebvre, B., Hunter, A. W., and Nohejlová, M. (2020b). Fossil weathering and preparation mimic soft tissues in eocrinoid and somasteroid echinoderms from the Lower Ordovician of Morocco. *Microscopy Today* 28 (1), 24–28. doi: 10.1017/S1515929519001238
- Saleh, F., Ma, X., Guenser, P., Mángano, M. G., Buatois, L. A., and Antcliffe, J. B. (2022b). Probability-based preservational variations within the early Cambrian Chengjiang Biota (China). *PeerJ* 10, e13869. doi: 10.7717/peerj.13869
- Saleh, F., Pittet, B., Perrillat, J.-P., and Lefebvre, B. (2019). Orbital control on exceptional fossil preservation. *Geology* 47 (2), 103–106. doi: 10.1130/G45598.1
- Saleh, F., Pittet, B., Sansjofre, P., Gueriau, P., Lalonde, S., Perrillat, J.-P., et al. (2020c). Taphonomic pathway of exceptionally preserved fossils in the Lower Ordovician of Morocco. *Geobios* 60, 99–115. doi: 10.1016/j.geobios.2020.04.001
- Saleh, F., Vaucher, R., Antcliffe, J. B., Daley, A. C., El Hariri, K., Kouraiss, K., et al. (2021b). Insights into soft-part preservation from the Early Ordovician Fezouata Biota. *Earth-Science Rev.* 213, 103464. doi: 10.1016/j.earscirev.2020.103464
- Saleh, F., Vaucher, R., Vidal, M., Hariri, K. E., Laibl, L., Daley, A. C., et al. (2022c). New fossil assemblages from the Early Ordovician Fezouata Biota. *Sci. Rep.* 12 (1), 20773. doi: 10.1038/s41598-022-25000-z
- Saleh, F., Vidal, M., Laibl, L., Sansjofre, P., Gueriau, P., Pérez-Peris, F., et al. (2021c). Large trilobites in a stress-free Early Ordovician environment. *Geological Magazine* 158 (2), 261–270. doi: 10.1017/S0016756820000448
- Saltzman, M. R., Young, S. A., Kump, L. R., Gill, B. C., Lyons, T. W., and Runnegar, B. (2011). Pulse of atmospheric oxygen during the late Cambrian. *Proc. Natl. Acad. Sci.* 108 (10), 3876–3881. doi: 10.1073/pnas.1011836108
- Servais, T., Owen, A. W., Harper, D. A. T., Kröger, B., and Munnecke, A. (2010). The Great Ordovician Biodiversification Event (GOBE): the palaeoecological dimension. *Palaeogeogr. Palaeoclimatol. Palaeoecol.* 294 (3–4), 99–119. doi: 10.1016/j.palaeo.2010.05.031
- Servais, T., Perrier, V., Danelian, T., Klug, C., Martin, R., Munnecke, A., et al. (2016). The onset of the 'Ordovician plankton revolution' in the late Cambrian. *Palaeogeogr. Palaeoclimatol. Palaeoecol.* 458, 12–28. doi: 10.1016/j.palaeo.2015.11.003
- Sieburth, J. M., Smetacek, V., and Lenz, J. (1978). Pelagic ecosystem structure: heterotrophic compartments of the plankton and their relationship to plankton size fractions 1. *Limnol. oceanography* 23 (6), 1256–1263. doi: 10.4319/lo.1978.23.6.1256
- Solé, V. A., Papillon, E., Cotte, M., Walter, P., and Susini, J. (2007). A multiplatform code for the analysis of energy-dispersive X-ray fluorescence spectra. *Spectrochimica Acta Part B: Atomic Spectrosc.* 62 (1), 63–68. doi: 10.1016/j.sab.2006.12.002
- Sun, Z., Zeng, H., and Zhao, F. (2020a). A new middle Cambrian radiodont from North China: implications for morphological disparity and spatial distribution of hurdiids. *Palaeogeogr. Palaeoclimatol. Palaeoecol.* 558, 109947. doi: 10.1016/j.palaeo.2020.109947
- Sun, Z., Zeng, H., and Zhao, F. (2020b). Occurrence of the hurdiid radiodont *Cambroaster* in the middle Cambrian (Wuliuan) Mantou Formation of North China. *J. Paleontol.* 94 (5), 881–886. doi: 10.1017/jpa.2020.21
- Vannier, J., Vidal, M., Marchant, R., El Hariri, K., Kouraiss, K., Pittet, B., et al. (2019). Collective behaviour in 480-million-year-old trilobite arthropods from Morocco. *Sci. Rep.* 9 (1), 14941. doi: 10.1038/s41598-019-51012-3
- Van Roy, P., and Briggs, D. E. G. (2011). A giant Ordovician anomalocaridid. *Nature* 473 (7348), 510–513. doi: 10.1038/nature09920
- Van Roy, P., Briggs, D. E. G., and Gaines, R. R. (2015a). The Fezouata fossils of Morocco; an extraordinary record of marine life in the Early Ordovician. *J. Geological Soc.* 172 (5), 541–549. doi: 10.1144/jgs2015-017
- Van Roy, P., Daley, A. C., and Briggs, D. E. G. (2015b). Anomalocaridid trunk limb homology revealed by a giant filter-feeder with paired flaps. *Nature* 522 (7554), 77–80. doi: 10.1038/nature14256
- Van Roy, P., Orr, P. J., Botting, J. P., Muir, L. A., Vinther, J., Lefebvre, B., et al. (2010). Ordovician Faunas of Burgess Shale type. *Nature* 465 (7295), 215–218. doi: 10.1038/nature09038
- Van Roy, P., and Tetlie, O. E. (2006). A spinose appendage fragment of a problematic arthropod from the Early Ordovician of Morocco. *Acta Palaeontologica Polonica* 51 (2), 239–246.
- Vaucher, R., Martin, E. L. O., Hormière, H., and Pittet, B. (2016). A genetic link between Konzentrat- and Konservat-Lagerstätten in the Fezouata Shale (Lower Ordovician, Morocco). *Palaeogeogr. Palaeoclimatol. Palaeoecol.* 460, 24–34. doi: 10.1016/j.palaeo.2016.05.020
- Vaucher, R., Pittet, B., Hormière, H., Martin, E. L. O., and Lefebvre, B. (2017). A wave-dominated, tide-modulated model for the Lower Ordovician of the Anti-Atlas, Morocco. *Sedimentology* 64 (3), 777–807. doi: 10.1111/sed.12327
- Vidal, M. (1998). Le modèle des biofaciès à trilobites: un test dans l'Ordovicien Inférieur de l'Anti-Atlas, Maroc. *Comptes Rendus l'Académie Des. Sciences-Series IIA-Earth Planetary Sci.* 327 (5), 327–333. doi: 10.1016/S1251-8050(98)80051-7
- Vinther, J., Stein, M., Longrich, N. R., and Harper, D. A. T. (2014). A suspension-feeding anomalocarid from the early Cambrian. *Nature* 507 (7493), 496–499. doi: 10.1038/nature13010
- von Siebold, C. T. E. (1848). *Lehrbuch der vergleichenden anatomie* (Berlin, Germany, Veit).
- Walcott, C. D. (1911). Cambrian Geology and paleontology II: middle Cambrian Holothurians and Medusae. *Smithsonian Miscellaneous Collections* 57 (3), 41–69.
- Walcott, C. D. (1912). Middle Cambrian Branchiopoda, Malacostraca, Trilobita, and Merostomata. *Smithsonian Misc. Collect.* 57 (6), 145–228.
- Whalen, C. D., and Briggs, D. E. G. (2018). The Palaeozoic colonization of the water column and the rise of global nekton. *Proc. R. Soc. B: Biol. Sci.* 285 (1883), 20180883. doi: 10.1098/rspb.2018.0883
- Whittington, H. B. (1975). The enigmatic animal *Opabimia regalis*, middle Cambrian, Burgess Shale, British Columbia. *Philos. Trans. R. Soc. London. B Biol. Sci.* 271 (910), 1–43. doi: 10.1098/rstb.1975.0033
- Wu, Y., Pates, S., Ma, J., Lin, W., Wu, Y., Zhang, X., et al. (2022). Addressing the Chengjiang conundrum: a palaeoecological view on the rarity of hurdiid radiodonts in this most diverse early Cambrian Lagerstätten. *Geosci. Front.* 13 (6), 101430. doi: 10.1016/j.gsf.2022.101430
- Zeng, H., Zhao, F., Yin, Z., and Zhu, M. (2017). Morphology of diverse Radiodontan head sclerites from the early Cambrian Chengjiang Lagerstätten, South-West China. *J. Syst. Palaeontol.* 16 (1), 1–37. doi: 10.1080/14772019.2016.1263685
- Zhu, X., Lerosey-Aubril, R., and Ortega-Hernández, J. (2021). Furongian (Jiangshanian) occurrences of radiodonts in Poland and South China and the fossil record of the Hurdiidae. *PeerJ* 9, e11800. doi: 10.7717/peerj.11800